Geosynthetics in Pavement Reinforcement Applications

Steven W. Perkins
Montana State University

Barry R. Christopher
Christopher Consultants

Nicholas Thom
University of Nottingham

Guillermo Montestruque
Consultant

Leena Korkiala-Tanttu
Pöyry Infra Oy

Arnstein Watn
SINTEF

Keywords: geosynthetic, pavement, reinforcement, subgrade, base, asphalt, modeling

ABSTRACT: The purpose of this paper is to review and present recent results of research pertinent to various applications of geosynthetics for reinforcement of roadway pavements. Applications discussed include subgrade stabilization, base reinforcement and asphalt reinforcement. Particular emphasis is placed on the mechanisms in operation for each application, a demonstration of pavement performance and benefit from the reinforcement layer in full-scale tests, and geosynthetic material properties and tests pertinent to the application. A discussion of performance tests, such as beam tests, wheel tracking tests and cracking tests, for asphalt reinforcement is presented. Recent activities in the area of numerical modeling and design of pavements are discussed. Models that fall within the category of mechanistic-empirical methods are highlighted.

1 INTRODUCTION

In this paper, applications of geosynthetics for reinforcement of roadway pavements are reviewed and discussed. These applications include subgrade stabilization, base reinforcement and asphalt reinforcement. Subgrade stabilization refers to situations where geosynthetics are placed on weak subgrade prior to the placement of an aggregate layer. The reinforced unpaved road may be used as is or may serve as a construction platform for a permanent paved road. Base reinforcement is used for permanent paved roads and is typically applicable for low volume roads founded on weak subgrade. Reinforcement placed within asphalt layers are used to reduce fatigue, thermal and reflective cracking, control rutting and mitigate the effects of frost heave.

For each application, full-scale field trials have demonstrated the benefit of the reinforcement. Given the multitude of high-quality field trials performed, only a sampling are presented in this paper to provide for adequate demonstration.

For purposes of design and specification, geosynthetic properties and the tests needed to define those properties are of great importance. A review of these properties and test methods is presented. Many of these tests have recently been developed to match the needs of these particular applications.

In the end, field demonstrations and test methods are of little use without tools with which engineers can use for design. Significant work has recently occurred in the development of design methods based on rigorous numerical models. These models and resulting design methods are presented and discussed.

2 SUBGRADE STABILIZATION

Geosynthetics are placed on weak, often saturated subgrades in combination with a granular layer to stabilize the subgrade and to provide a working platform for construction of unpaved roads and either flexible or rigid pavement systems. The granular layer may be the base or subbase component of the pavement system or it may be additional gravel required to support initial construction and not considered as part of the pavement section. Soft, weak subgrade soils provide very little lateral restraint. When roadway aggregate moves or shoves laterally, vertical deformation occurs and ruts develop on the aggregate surface. A geogrid with good interlocking capabilities or a geotextile with good frictional capabilities can provide *reinforcement* in the form of tensile resistance to lateral aggregate movement. The reinforcement provides lateral restraint and initiates increased horizontal stress on the aggregate, thus reducing the mobilization of the soil and reducing plastic deformations (i.e., reduced rutting). The geo-

synthetic also increases the system bearing capacity by forcing the potential bearing surface under the wheel load to develop along an alternate, longer mobilization path and thus higher shear strength surfaces.

Other functions of the geosynthetic play an equally, if not more important, role in this application. The geosynthetic must provide *separation* to prevent intermixing of the granular material and the subgrade. Only a small amount of fines penetrating into the granular layer will negatively affect its structural characteristics (i.e., reduced shear strength, lowered permeability and increased frost susceptibility). Separation is provided directly by geotextiles or by composite geosynthetics. Geotextiles perform this function by preventing penetration of the aggregate into the subgrade (localized bearing failures) and prevent intrusion of subgrade soils up into the base course aggregate. Geogrids can also prevent aggregate penetration into the subgrade, depending on the ability of the geogrid to confine and prevent lateral displacement of the base/subbase. However, the geogrid does not prevent intrusion of subgrade soils up into the base/subbase course and the granular layer used with the geogrid must provide this function or a geotextile must be used in combination with the geogrid.

The subgrade soils in this application are fine grained soil with a high water content. The geotextile, whether the primary stabilization geosynthetic or a separation layer used with a geogrid, must also provide filtration to allow excess pore water pressure to dissipate into the aggregate base course and, in cases of poor-quality aggregate, through the geotextile plane itself. In the case of geogrids, the granular layer supported by the geogrid must have a gradation that is compatible with the subgrade, based on standard geotechnical graded granular filter criteria. It is the reinforcement, separation, filtration and drainage functions that combine to provide the mechanical stabilization for weak subgrade soils (Holtz, et al., 2008).

Geosynthetics are primarily used in stabilization applications to facilitate construction. Even if the finished roadway can be supported by the subgrade, it may be virtually impossible to begin construction of the embankment or roadway without some form of stabilization. Geosynthetics offer a cost-effective alternative to other expensive foundation stabilization methods such as dewatering, demucking, excavation and replacement with select granular materials, utilization of thicker stabilization aggregate layers, or chemical stabilization. This mechanically stabilized layer also enables contractors to meet minimum compaction specifications for the first two or three aggregate lifts.

While the stabilization application is primarily used for initial construction, geosynthetics also provide long-term benefits and improve the performance of the road over its design life. The geosynthetic continues to perform by maintaining the roadway design section and the base course material integrity by preventing the aggregate from penetrating the subgrade. In addition, the separation function provided by geotextiles, geogrid/geotextile geocomposites or geogrids with appropriately designed filter aggregate prevent the migration of fines into base/subbase materials, especially into open graded bases, maintaining the support and drainage characteristics of the base over the life of a pavement system. In essence, the geosynthetic improves the reliability of the pavement system performance, especially during overload and/or seasonally weak subgrade conditions. Thus, the geosynthetic should ultimately increase the life of the roadway.

2.1 Mechanisms of reinforcement

The two primary mechanisms with this application are increased bearing capacity and lateral restraint, both of which significantly contribute to load-carrying capacity. When an aggregate layer is loaded by a vehicle wheel or dozer track, the aggregate tends to move or shove laterally and is restrained by the subgrade or geosynthetic reinforcement, a pavement reinforcement mechanism (Figure 1a). Components of this mechanism include: (i) restraint of lateral movement of base, or subbase, aggregate (confinement); (ii) increase in modulus of base aggregate due to confinement; (iii) improved vertical stress distribution on subgrade due to increased base modulus; and (iv) reduced shear strain along the top of the subgrade. In addition, the geosynthetic reinforcement forces the potential bearing capacity failure surface below the wheel load, which is analogous to a footing on foundation soil, to follow an alternate higher strength path as shown in Figure 1b. This tends to increase the bearing capacity of the subgrade soil.

A third possible geosynthetic reinforcement function is membrane-type support of wheel loads, as shown conceptually in Figure 1c. In this case, the wheel load stresses must be great enough to cause plastic deformation and ruts in the subgrade. If the geosynthetic has a sufficiently high tensile modulus, tensile stresses will develop in the reinforcement, and the vertical component of this membrane stress will help support the applied wheel loads. As tensile stress within the geosynthetic cannot develop with-

out some elongation, wheel path rutting (in excess of 100 mm as determined by Giroud and Noriay, 1981) is required to develop membrane-type support. Therefore, this mechanism is generally limited to temporary roads or the first aggregate lift in permanent roadways, if significant rutting can be tolerated. These reinforcement mechanisms were originally described by Bender and Barenberg (1978) and later elaborated on by Kinney and Barenberg (1982) for geotextile-reinforced unpaved roads.

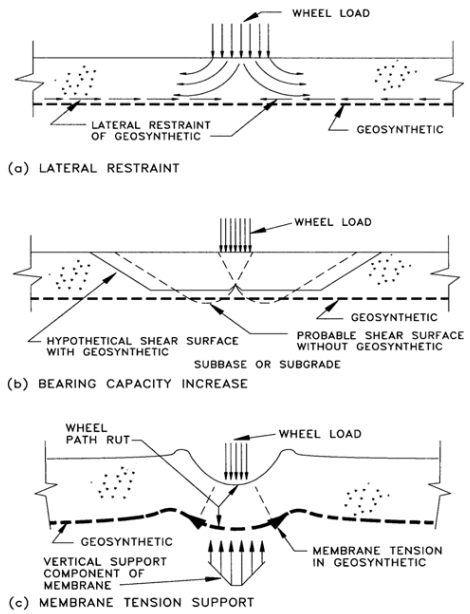

Figure 1. Possible reinforcement functions provided by geosynthetics in roadways: (a) lateral restraint, (b) bearing capacity increase, and (c) membrane tension support (Holtz et al, 2008, after Haliburton, et al., 1981).

The influence of each reinforcement mechanism will diminish with stronger subgrade conditions and as additional layers of base and the pavement system are placed. The effect of the reinforcement also increases with increasing acceptable deformation (rutting). As previously indicated, when little or no rutting of the subgrade occurs, the membrane tension support does not exist. Also, with stronger subgrades, bearing capacity is not an issue and lateral movement of the gravel under construction equipment diminishes. Research indicates that stabilization for construction is generally no longer required for subgrade soils with a soaked CBR value approximately greater than three to four (CBR < 3 to 4), shear strengths greater than approximately 90 to 120 kPa, and resilient modulus greater than approximately 30 to 40 MPa. From a foundation engineering point of view, clay soils with undrained shear strengths of 2000 psf (90 kPa) or higher are considered to be stiff clays (Terzaghi and Peck, 1967) and are generally quite good foundation materials. Simple stress distribution calculations show that for static loads, such soils will readily support reasonable truckloads and tire pressures, even under relatively thin granular bases.

As the thickness of the gravel layer increases or stiffer components of the pavement section are added, the stress at the geosynthetic decreases to a point where there is little or no geosynthetic deformation and correspondingly little or no reinforcement. The actual thickness where this occurs is related to the subgrade strength, the type and magnitude of the wheel load, and the number of vehicle passes. Thus design solutions should evaluate each of these elements.

Again, the reinforcing function can be compromised if separation and filtration are not provided. Several case histories have documented poor performance of reinforcements, when the separation function was not achieved. For example, the US Army Corps of Engineers District in Baltimore documented a subgrade restraint failure due to separation problems in a test strip pilot study to evaluate optimal subgrade stabilization (US Army Corps of Engineers, 1999). Severe rutting and localized bearing failures were attributed to intermixing between the subgrade soils and a well graded granular base in a test section where a geogrid was placed directly on the subgrade. Separate test strips under the same conditions found that a stabilization geotextile performed adequately with some rutting and a geogrid over a separation geotextile performed with minimal rutting. Another indication of the importance of these functions is the number of research studies that have identified varying performance by different geosynthetics as discussed in the next section on full scale performance.

2.2 Full Scale Performance

The use of geotextiles for subgrade stabilization to solve problems encountered in constructing unpaved and paved (both flexible and rigid pavements) roads over soft, wet subgrades was well established internationally in the 1970s. The performance of geosynthetics used in stabilization applications in low-volume roads have been well documented in numerous case histories, full-scale laboratory experiments, and instrumented field studies, some of which include Steward et al. (1977), Bender and Barenberg, (1978), Haliburton and Barron (1983), Haas et al. (1988), Austin and Coleman (1993), Tsai (1995),

Fannin and Sigurdsson (1996), Knapton and Austin (1996), Hayden et al. (1999), Gabr et al. (2001), Leng and Gabr (2002), Tingle and Webster (2003), Hufenus et al. (2004), Watts et al. (2004), Christopher and Lacina (2008), and Christopher and Perkins (2008). Summaries of much of this research is contained in Berg et al. (2000), Christopher et al. (2001), Watn et al. (2005) and in the European study Cost 348 WG1 (2004).

As indicated in the previous section, the results of these studies vary in terms of the performance of different geosynthetic types. For example, in some studies geogrids were found to perform better than geotextiles (e.g., Barksdale et al., 1989); in some studies, geotextile and geogrid performance has been found to be essentially the same (e.g., Fannin and Sigurdsson, 1996 and Hayden et al. 1999); in others, geotextiles were found to perform better than geogrids (Al-Qadi et al., 1994 and Christopher and Lacina, 2008); and in all cases, where composite geogrid/geotextile systems were used, they always performed the best (Fannin and Sigurdsson, 1996, Christopher and Perkins, 2008, and Christopher and Lacina, 2008). Recent work by Christopher et al. (2009) has found that these varying results may be due to pore water pressure development in the subgrade and the ability for the pore water pressure to dissipate during loading.

In full scale laboratory tests performed to evaluate geosynthetics used in both stabilization and base reinforcements on a number of different geosynthetics in several separate studies (Perkins et al., 2004, Christopher and Lacina, 2008, and Christopher et al., 2009) have observed the development and increase of pore water pressure measured in the wet, nearly saturated subgrade during cyclic loading. As indicated in these references and the representative results shown in Figure 2 and Figure 3, the pore water pressure measurements in most of the tests were found to directly correspond to the performance of the geosynthetic. The largest amount of deformation per cycle was found to occur in the tests with the highest developed pore pressure (e.g., the control tests in Figure 2) and the best performing tests (least amount of rutting under the same number of cycles) were in the sections with the lowest measured pore pressure (e.g., see Figure 2). The full scale studies found that the reinforcement action of an open geogrid positively results in lower pore water pressure development than measured in control tests (i.e., with no geosynthetics) performed on the same subgrade (e.g., GG_{ex} and GG_{w} in Figure 2). The addition of a nonwoven geotextile to the reinforcement geogrid provides additional separation and filtration features that further limit the development of excess pore water pressure and significantly further reduces rutting (e.g., Figure 3). These results also indicate that geotextiles with better filtration and drainage characteristics (e.g., GT_{w2} and GT_{w3} in Figure 2) tend to perform better with wet silt and clay type soils than geotextiles with low permeability or permittivity (e.g., GT_{w1} in Figure 2) as well as open geogrids, where separation performance was questionable.

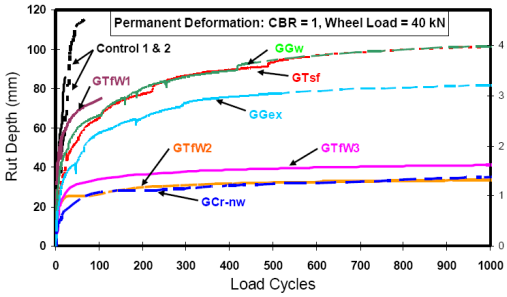

(a) deformation response for geosynthetics on silt subgrade

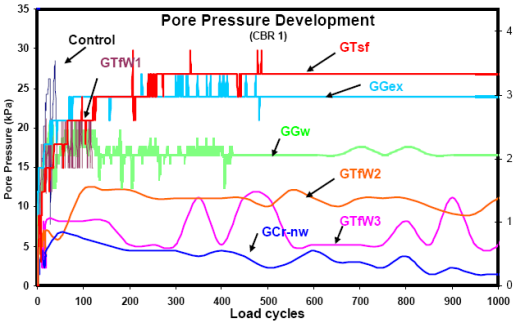

(b) pore water pressure measurements in subgrade

Figure 2. Representative results from full scale laboratory stabilization tests with subgrade pore pressure measurements (Christopher and Lacina, 2008)

These results indicate that the performance of the geosynthetics varies with both the subgrade type and conditions (i.e., a geosynthetic may perform well in one condition and not so well under other conditions). Geosynthetics could influence the development and magnitude of pore water pressure through: 1) a reduction in stress in the subgrade (Berg et al., 2000); 2) separation, which would reduce point stress and corresponding pore pressure developed from gravel penetration into subgrade layers (Christopher and Lacina, 2008); and/or, 3) pore pressure dissipation in the plane of some geosynthetics when the in plane permeability is greater than the permeability of the base layer (e.g., poorly draining base layers containing fine grained soils) (Holtz et al., 2008).

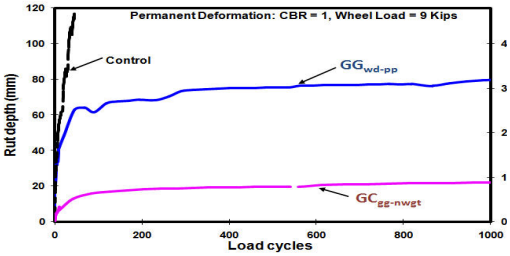

(a) deformation response for geogrids on silt subgrade

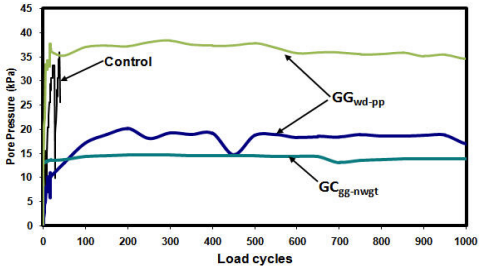

(b) pore water pressure measurements in subgrade

Figure 3. Representative results from full scale laboratory stabilization tests on geogrids and silt type subgrade with pore pressure measurements (Christopher and Perkins, 2009)

Most of these studies are focused on short-term (i.e., during construction and initial traffic) performance. Several studies are currently underway to monitor long-term performance. Full scale test sections constructed by the Maine DOT had several test sections using stabilization geotextiles for comparison with the geogrid base reinforcement test sections (Hayden et al. 1999). Stabilization aggregate required in the control section was eliminated in all of the geosynthetic test sections. Monitoring of a Washington DOT pavement test section in which separation/stabilization geotextiles were used is anticipated to be continued over the full pavement design life (Black and Holtz 1997). Al-Qadi and Appea (2003) also reported on an eight year study investigating the effects of geogrid and geotextile reinforcement placed between the base course and subgrade. In the first eight years of performance, only the thinnest, 100 mm thick base course has realized a measurable increase in service life and pavement quality. A stabilization research project is currently being conducted by the University of Wisconsin in cooperation with the Wisconsin DOT, in which geosynthetic stabilization test sections are being compared with sections stabilized using fly ash and bottom ash (Woon-Hyung et al., 2005). The geosynthetic sections are instrumented, strain gages are mounted on the geosynthetics and a control section was installed. The Geosynthetic Research Institute (GRI) has an ongoing study to monitor test sections where geosynthetics have been used as separators (GRI, 2001). Although the study is focused on the long-term benefits of geotextile separators, in many of the projects that are being monitored, geosynthetics were initially used for subgrade stabilization. A database of full-scale field test sites has been developed and is maintained at GRI. Monitoring is proposed for up to 20 years.

2.3 Geosynthetic Material Properties and Tests

As with any geosynthetic application, the material properties required for design are based on: 1) the properties required to perform the primary and secondary function(s) for the specific application over the life of the system, and 2) the properties required to survive installation. The separation and filtration functions are related to opening characteristics and are determined based on the gradation of the adjacent layers (i.e., subgrade, base and/or subbase layers). Some strength is, of course, required for the reinforcing function, which is based on the requirements in the specific design approach. If the roadway system is designed correctly, then the stress at the top of the subgrade due to the weight of the aggregate and the traffic load should be less than the bearing capacity of the soil times a safety factor, which is generally a relatively low value compared to the strength of most geosynthetics. However, the stresses applied to the subgrade and the geotextile during construction may be much greater than those applied in-service. Therefore, the strength of the geotextile or geogrid in roadway applications is usually governed by the anticipated construction stresses and the required level of performance. This is the concept of geosynthetic survivability -- the geosynthetic must survive the construction operations if it is to perform its intended function. In fact, for subgrade stabilization, the geosynthetic survivability tends to control the strength requirements and not the reinforcement function.

In the US, the Federal Highway Administration (FHWA) (Holtz et al, 2008) and the American Association of Highway and State Transportation Officials (AAHSTO) (AASHTO M288, 2006) provide tables specifically for stabilization applications that relate geosynthetic index properties defined by the American Society for Testing and Materials (i.e., grab strength, CBR puncture resistance, and tear resistance for geotextiles; and, wide width strength and strength for geogrids) to survivability of geosynthetics. The geosynthetics are classified as High (Type 1), Moderate (Type 2) and Low (Type 3) survivability geosynthetics and the types are matched to specific installation conditions. Opening character-

istics for geogrids based on the relation to the granular layer particle size and for geotextiles based on separation and filtration requirements are also included in the tables plus permittivity requirements are specified for geotextiles.

A similar approach has been developed in the Nordic countries of Finland, Sweden and Norway through the establishment of the NorGeoSpec system in 2002 (Moe, 2008). This is a certification scheme (specification and control) for geotextiles used for separation, filtration and stabilization in roads. The system includes five specification profiles based on several characteristics measured with test methods defined by the Central European Normalization (CEN) and the International Standards Organization (ISO). Classification of the geotextiles in a specific profile is based on test values and tolerances for the following characteristics: tensile strength, tensile strain, strain energy index, static puncture, dynamic perforation resistance, characteristic opening size and permeability.

In Denmark, the road design procedure equally requires that the geosynthetic be flexible and strong enough to withstand stresses from the surrounding gravel or rocks without being damaged. The requirement for the geotextiles could be based on a design model such as that proposed by Steen (2004).

Other properties, such as stiffness, aperture size and interlock effect, may be required for the specific design method as discussed in Section 5.2. Almost no correlations have been developed between properties and field performance of geosynthetics in subgrade stabilization applications. In order to develop such correlations, Berg et al, 2000 has recommended that the following properties of interest be provided with any future full scale studies or long-term pavement studies: 2% & 5 % secant moduli, Coefficient of Pullout Interaction, Coefficient of Direct Shear, Aperture Size, and Percent Open Area. A proposal for guidelines for reinforcement in road structures in Norway emphasizes the necessity of linking the reinforcement function to the dominating deterioration mechanisms. The required reinforcement properties are then given based on an evaluation of different deterioration mechanisms. Generally the required properties can be grouped into strength and stiffness, interaction properties with surrounding material and survivability (Øiseth and Hoff, 2006).

3 BASE REINFORCEMENT

In this paper, base reinforcement refers to the placement of geosynthetics within the unbound aggregate base layer of a paved flexible pavement for the purpose of improving the permanent deformation (rutting) and fatigue cracking performance of the pavement during its operational life. While the mechanisms and benefits of base reinforcement occur in unpaved roads, the focus of the material presented in this section is on paved roads.

The application of a vehicular load to a flexible pavement results in dynamic stresses within the various pavement components. The stiffness of these components dictates the magnitude of the dynamic strains and displacements, which are small in a well-designed pavement. As vehicular loads are repeatedly applied, permanent strain is induced and accumulates as traffic passes grow, which leads to rutting of the pavement surface. Fatigue cracking of the asphalt concrete layer also results from repeated cycles of tensile lateral strain in the bottom of the layer.

Relatively small dynamic strains and the accumulation of permanent strain points to several important considerations when using geosynthetics for reinforcement. Small-strain stiffness as opposed to strength at large levels of strain is important for characterizing the geosynthetic. Many applications developed for large strain failure analysis, so this has caused a shift in thinking and testing.

3.1 *Mechanisms of Reinforcement*

The overriding mechanism of reinforcement is one in which the reinforcement prevents lateral movement of the base aggregate through shear interaction between the base and the geosynthetic. This has the effect of increasing the confinement or mean stress in the aggregate in the vicinity of the geosynthetic. Aggregate materials have a resilient modulus that is mean stress dependent, meaning that as the confinement increases, the stiffness of the aggregate increases.

Lateral restraint of the aggregate occurs during both construction of the roadway and during traffic loading. During construction, heavy compaction equipment applies large compressive stresses to the granular layers. The motion of aggregate during compaction is complex yet involves a significant component in the lateral direction. For unreinforced aggregate, Mooney and Reinhart (2009) showed compressive vertical strain and horizontal extension in the direction of travel of a drum roller (Figure 4), where stresses and strains are due to the compactor and relative to the geostatic condition. The horizontal extension strain in the direction of drum travel is similar in shape to that seen when a vehicular wheel load is applied and is explained by heavy direct loading in the vertical (z) direction, moderate confinement in the direction perpendicular to drum travel (y) and light confinement in the direction of drum travel (x). Horizontal strain in the direction perpendicular to drum travel was seen to be very small, indicating that nearly plane strain conditions exist beneath the roller during compaction.

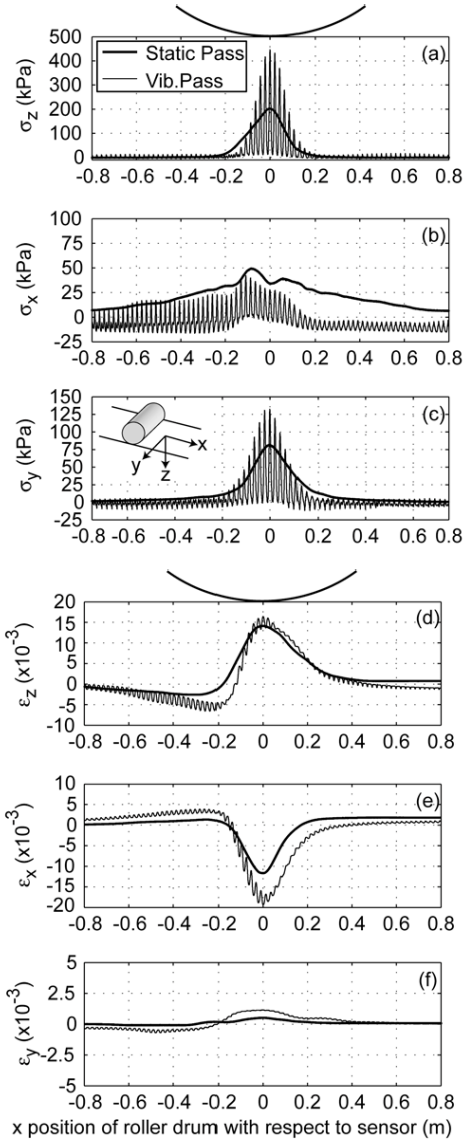

Figure 4. Stresses and strains induced in compacted aggregate beneath a drum roller (Mooney and Reinhart 2009).

Residual stress in the lateral direction of the compacted aggregate is locked in. Several studies have shown locked-in horizontal stress as high as 35 kPa due to compaction and application of wheel loads (Uzan 1985, Selig 1987 and Barksdale & Alba 1993). D'Appolonia et al. (1969) showed values of the coefficient of earth pressure at rest (K_o) in terms of static locked-in horizontal stresses due to vibratory compaction, to be between 0.8 and 1.1 and increased with increasing compaction passes. Duncan and Seed (1986) and Duncan et al. (1991) also discussed and modeled locked-in horizontal stress. Brandl et al. (2005) and Mooney and Reinhart (2009) showed that in unreinforced aggregates, static passes resulted in locked-in horizontal stresses while vibratory passes tend to release these stresses.

When reinforcement is present, lateral restraint of aggregate occurs through shear interaction between the aggregate and the geosynthetic as aggregate experiences lateral extensional strain. During compaction, Figure 4 shows that lateral extensional strain occurs principally in the longitudinal (x) direction, which implies that the stiffness of the reinforcement in this same direction is of most importance. During traffic loading when extensional strains are greatest in the transverse (y) direction, reinforcement stiffness in this direction will be more important. Reinforcement may also be effective in preventing the release of locked-in horizontal stress during vibratory compaction.

Konietzky et al. (2004) used a discrete element modeling (DEM) method with a 3D particle flow code to numerically describe locked-in horizontal stresses due to compaction and traffic loading. The DEM method has advantages to continuum based numerical methods in that it has the potential to describe complex interactions between discontinuous combinations of aggregate and geosynthetics. The method was used to apply a vertical consolidation pressure, representing a compaction load, to a column of aggregate with a geogrid layer. The horizontal stress in the aggregate was determined after the consolidation pressure was removed and was shown to be approximately twice as large as compared to a case where no geogrid was present. The application of shear load between the geogrid and the aggregate also resulted in additional locked-in horizontal stress.

DEM studies have provided a numerical means of confirming experimental results discussed above, have provided additional evidence for the mechanism of lateral restraint, and have supported earlier mechanistic-empirical design methods proposed by Perkins et al. (2004) and described in Section 5 of this paper, which rely upon the mechanism of lateral restraint. The complexity of the DEM method and the long run times associated with the computations limit it presently to use for fundamental research, which are anticipated to provide guidance for anticipated levels of locked-in stresses predicted and used in design based numerical models for reinforced pavements.

Lateral restraint of aggregate also occurs during traffic loading. Similar to the operation of compaction equipment, vehicular loads applied to the roadway surface create a lateral spreading motion of the base course aggregate as illustrated schematically in Figure 5. Extensional lateral strains are created in the base below the applied load as base material moves down and out away from the load centerline.

Figure 6 shows data from instrumented pavement box tests illustrating extensional lateral strain out to a radius of approximately 200 mm, where after compressive strains are seen.

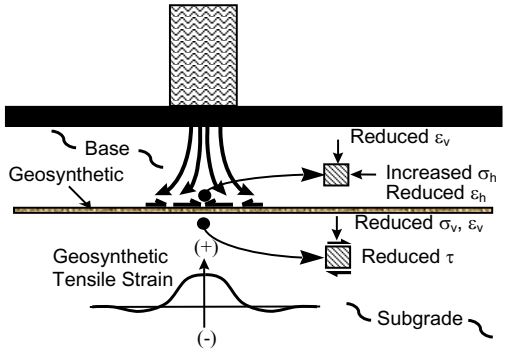

Figure 5. Mechanisms of reinforcement

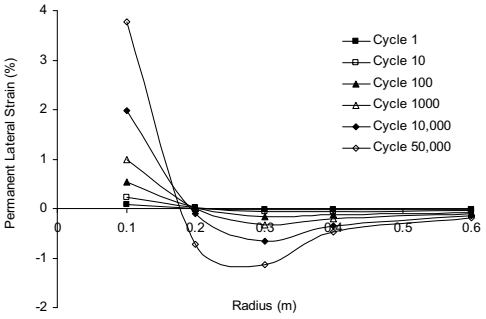

Figure 6. Permanent lateral strain at the bottom of base aggregate in an unreinforced test section (Perkins 1999).

The motion of aggregate illustrated in Figure 5 and Figure 6 results in tensile load being transferred to the geosynthetic by shear interaction between the aggregate and the geosynthetic. This in turn results in a tensile strain distribution in the geosynthetic as schematically shown in Figure 5, which has been shown experimentally in several pavement studies (Haas et al. 1988, Miura et al. 1990, Perkins et al. 1998a,b and Perkins 1999) and is shown in Figure 7 for the Perkins (1999) study. The data shows permanent tensile strain out to a radius of approximately 250 mm and shows the strain to grow with increased trafficking of the section.

The thickness of aggregate over which lateral restraint occurs is important from the standpoint of understanding how much of the aggregate layer receives a stiffening effect from the reinforcement. Using results from DEM studies, Kwon et al. (2008) conclude that approximately 150 mm of aggregate is influenced for pure vertical loading and 50 mm for pure shear loading. Eiksund et al. (2004) conducted large-scale repeated load triaxial tests on aggregate with a layer of reinforcement and showed that lateral strain was restrained within a zone of 150 mm above the reinforcement.

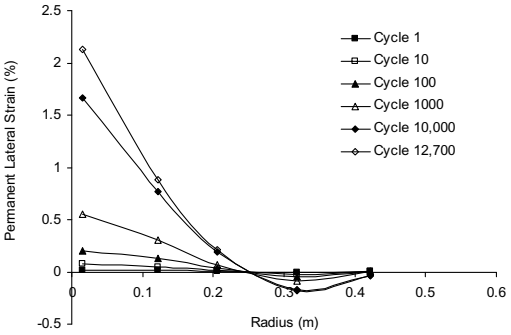

Figure 7. Geosynthetic strain distribution (Perkins 1999).

Once lateral restraint of aggregate occurs and a stiffening of the aggregate is seen, the pavement layers respond by mechanisms further illustrated in Figure 5. Compressive stress is reduced on the subgrade. Shear stress transmitted from the base course to the subgrade decreases as shearing of the base transmits tensile load to the reinforcement. Less shear stress, coupled with less vertical stress results in a less severe state of loading (Houlsby and Jewell, 1990) leading to lower vertical strain in the subgrade. Finally, reduced vertical strain in the base and subgrade results in less surface deflection, which results in less dynamic tensile strain in the bottom of the asphalt concrete layer and a greater fatigue life.

3.2 *Full-Scale Performance*

Construction, traffic loading and monitoring of full-scale base-reinforced test sections has been critically important for demonstrating the feasibility of the technology, understanding the conditions under which reinforcement benefit is seen, describing the magnitude of this benefit, understanding the mechanisms by which reinforcement occurs and providing data to which research and design models can be compared. The construction of base-reinforced test sections has been an on-going activity for nearly 30 years and has taken many forms ranging from laboratory-based test sections to demonstration projects constructed on public roadways. Several synthesis reports have been prepared (Berg et al. 2000, Christopher et al. 2002, Al-Qadi et al. 2009), which describe work performed in this area.

Paved roads are considered to be inoperable once large surface deformations are seen. Most studies have therefore focused on paved road performance and improvements offered by geosynthetics for pavement deformation less than 25 mm. A number of studies have demonstrated that the service life of the pavement, as defined by the number of load

repetitions carried by the pavement to reach a particular permanent surface deformation, can be increased by a factor ranging from just over one to in excess of 100 by the inclusion of a geosynthetic in the base aggregate layer. Studies have also shown that base course thickness can be reduced by up to 50 % by the inclusion of a geosynthetic. Most studies have quantified benefit in terms of rutting. Benefit defined in terms of increased fatigue life of the asphalt concrete layer has been more difficult to demonstrate experimentally and is needed to verify these benefits predicted by reinforced pavement design models discussed in Section 5.1.

Berg et al. (2000) have given a comprehensive review of available studies, where the variables involved in the studies and the type and magnitude of benefit derived by the geosynthetic has been summarized. This document was used as the basis for an AASHTO standard (AASHTO 2001) providing a recommended practice for the use of geosynthetics as reinforcement in flexible pavements.

Two full-scale accelerated pavement tests have been conducted with a Heavy Vehicle Simulator (HVS) in Finland (Kangas et al. 2000) and one in Sweden (Pihlajamäki et al.2002) with the base layer reinforced with steel grid. The main objective of the tests was to find out the effect of the reinforcement on rutting.

The HVS test results showed that the depth of the rut can be remarkably reduced by using steel grids in unbound base (Korkiala-Tanttu et al. 2003a). On average, this reduction was between 40 – 60 %, which results in an increase of service life between 50 - 100 %.

The efficiency of the reinforcement depended on the conditions where it is used. The reinforcement worked best in cases where the bearing capacity of the pavement is low. If the bearing capacity of the pavement is high, reinforcement did not have much of an effect on rutting (Korkiala-Tanttu et al. 2003a).

Steel grids are commonly used in Finland and Sweden to reduce cracking caused by frost heaving. A steel grid prevents the development of longitudinal frost cracks in the reinforced area according to the test results reported by Kivikoski et al. (2002) and over twenty years of field experience with reinforced and unreinforced structures (Sandberg and Björnfot 2004). The longitudinal cracks usually move to the shoulder of the road where grid reinforcement ends. Steel grid also mitigates transverse frost cracking by curtailing the width of the cracks and by preventing the development of small cracks.

To prevent frost cracking the grid must be installed in the whole width of the road. No overlapping of the steel grid is needed in longitudinal direction to prevent frost cracks. On the contrary the space between adjacent grids can be up to 500 mm, if the frost heave is less than 100 mm (Kivikoski et al. 2002). If the frost heave is larger than 100 mm, the grids should be installed with an edge joint (close to each other with no space between them).

Test sections show that the frost heave differentials in the cross section can be reduced with steel grids (Kivikoski et al. 2002). The Reflex project recommends (Gustafson et al. 2002) that at least a 50 mm asphalt layer should be spread upon the steel grid.

Even though many field and full-scale tests show that reinforcement clearly improves the performance of a pavement, it has been difficult to show benefit with Falling Weight Deflectometer (FWD) measurements (Korkiala-Tanttu et al. 2003a). The surface moduli of a reinforced pavement measured with FWD were usually only slightly greater than the moduli of an unreinforced pavement, yet the difference between service lives showed significant improvement.

3.3 *Geosynthetic Material Properties and Tests*

Geosynthetic material properties and their corresponding test methods are critical for design and specification of reinforcement geosynthetics for base reinforcement. This is especially true for generic specifications and non-proprietary design methods, particularly those that involve mechanistic-empirical principles.

In general, it is recognized that tensile load-strain properties of the geosynthetic itself and geosynthetic-aggregate shear interaction properties are important for assessing the performance of the base-reinforced pavement. This follows from an understanding of reinforcement mechanisms described in Section 3.1, which imply that good interaction properties are necessary to transfer load from the aggregate to the reinforcement and that good load-strain properties of the geosynthetic are required to limit lateral movement of the aggregate. While engineering material properties describing load-strain and interaction behavior are important, Tang et al. (2008) has shown the problems associated with an attempt to correlate a single material parameter to reinforcement performance. In particular, Tang et al. (2008) showed an absence of clear correlation between index properties (including ultimate strength, tensile strength at 2 % strain, junction strength, aperture area and flexural rigidity) with performance of small-scale accelerated pavement tests. The study showed some correlation between interaction properties and performance. This indicates that no one single parameter can define performance and that parameters work together or against each other in determining how the reinforcement will benefit the pavement. In addition, tests traditionally carried out at large strains are not necessarily appropriate for this application, which involves small strains.

Material properties may be broadly classified as those needed for design and those needed for speci-

fication. For design purposes, the focus of this paper is on material properties that are pertinent to mechanistic-empirical design methods of the type described in Section 5.1. This method uses an axi-symmetric finite element model for the mechanistic response model. This model requires input properties for the reinforcement load-strain material model and the geosynthetic-aggregate shear-displacement interaction model.

Load-strain material models for the reinforcement should be similar in complexity to material models used for the other pavement components and consistent with the capabilities of an axi-symmetric model. The above is accomplished by using a simple isotropic linear elastic model for the reinforcement, which requires specification of an elastic tensile modulus and Poisson's ratio describing the elastic stress-strain behavior of the reinforcement. Geosynthetic reinforcement products, however, generally have a tensile modulus that is different in the two principal directions of the product. This implies that an orthotropic elastic model (a direction dependent model) is better suited to describe the reinforcement. This type of model, however, is not compatible with an axi-symmetric finite element model, which is direction independent within a horizontal plane occupying the reinforcement layer.

Perkins and Eiksund (2005) devised a method to convert orthotropic elastic properties of a reinforcement layer to an isotropic elastic modulus, E, for an assumed isotropic Poisson's ratio of 0.25 (Equation 1). Orthotropic properties include an elastic tensile modulus in the two principal directions of the material (E_m, E_{xm}), an in-plane Poisson's ratio (ν) and an in-plane shear modulus (G). In this equation, the constants a and b are 0.35 and 0.035. Three material tests are therefore required to determine these properties.

$$E = \frac{1 - 0.5a + a^2 + 2.5b^2}{\frac{1}{E_{xm}} + \frac{a^2}{E_m} - 2a\frac{\nu}{E_{xm}} + \frac{b^2}{G}} \qquad 1$$

Material laboratory tests used to describe properties of the reinforcement or properties of shear interaction between the reinforcement and aggregate should be capable of accounting for the small-strain/displacement and repetitive load conditions present in base-reinforced pavements. Cuelho et al. (2005) proposed a cyclic in-air tension test to describe the elastic tensile modulus of the reinforcement in its two principal directions and as a function of a set permanent strain. This was accomplished by statically loading a wide-width tensile specimen to a prescribed axial strain, followed by the application of 1000 load cycles where the axial strain varied between prescribed limits of +/- 0.1 % of the prescribed static strain. This was followed by applying additional static load to the specimen to bring it to a new and higher prescribed static strain, then followed by the cyclic load sequence. These steps were then repeated for a total of 6 steps as illustrated in Table 1. The tests performed in this way were cyclic stress-relaxation tests, in that load was allowed to decrease as the strain was cycled between set limits.

Table 1. Loading steps for cyclic in-air tension tests.

Step	Static Strain (%)	Cyclic Strain (%)
1	0.5	0.2
2	1.0	0.2
3	1.5	0.2
4	2.0	0.2
5	3.0	0.2
6	4.0	0.2

Figure 8 illustrates representative results for a test performed on a biaxial geogrid. This material is listed as geosynthetic E in Table 2. From this type of test, the tensile modulus is determined as the slope of the load-strain curve at the end of cyclic loading for each step. Figure 9 shows a summary of tensile modulus values for 3 geotextiles and 4 geogrids tested in the machine direction, where these products are listed in Table 2. The three geotextiles show an increase in modulus with increasing permanent strain level whereas the geogrids tested show a relatively constant value of modulus at all strain levels. Similar trends were observed for these materials when tested in the cross-machine direction. These results suggest that geotextiles of the type tested require some permanent strain, and hence rutting, before a stiff tensile response is seen.

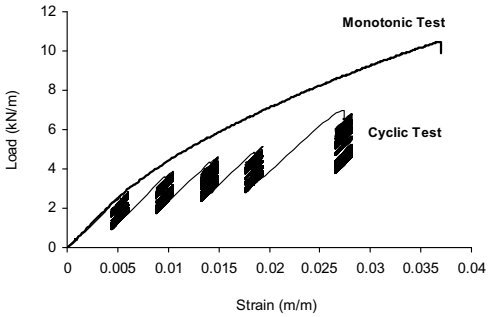

Figure 8. Cyclic in-air tension results for a biaxial geogrid (geosynthetic E).

The cyclic in-air tension test described above has been proposed as an ASTM standard (Determining Small-Strain Tensile Properties of Geogrids and Geotextiles by In-Air Cyclic Tension Tests) and is currently in the final stages of balloting. The standard calls for a strain rate during all phases of testing of 10 %/minute in order to conform to existing wide-width tension testing standards (ASTM 4595 and 6637). Further research is needed to evaluate the effect of cyclic strain rates more in line with those an-

ticipated in base-reinforcement applications, which may be as high as 500 to1000 %/min.

Table 2. Geosynthetic materials used for cyclic in-air tests

Geosynthetic Type	Manufacturer & Brand Name	Generic Name	Polymer Type / Structure
Geotextile	Amoco ProPex 2006	A	PP / woven
	Synthetic Industries Geotex 3×3	B	PP / woven
	Ten Cate Nicolon Geolon HP570	C	PP / woven
Geogrid	Colbond Enkagrid Max 20	D	PP / welded grid
	Tensar BX1100	E	PP / biaxial, punched, drawn
	Tensar BX1200	F	PP / biaxial, punched, drawn
	Tenax MS220b	G	PP / extruded, multi-layer

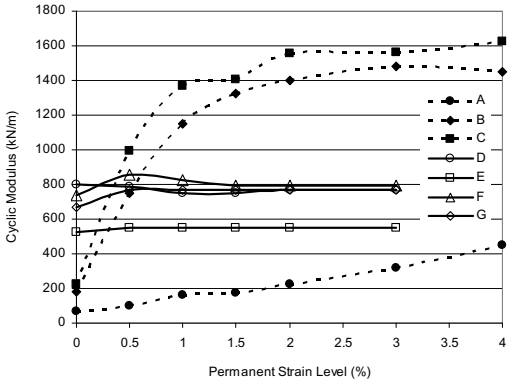

Figure 9. In-air tension results for 7 geosynthetics, machine direction.

Biaxial tension tests similar to those described by McGown and Kupec (2004) can be used to determine Poisson's ratio. Hangen et al. (2008) noted several problems and solutions for the test proposed by McGown and Kupec (2004). Perkins et al. (2004) proposed equations for evaluating Poisson's ratio (ν) from biaxial tests performed as equal rate of loading tests (Equation 2) and as equal rate of strain tests (Equation 3).

$$\nu = \frac{E_{xm-U}}{E_{m-B}}\left(\frac{E_{m-B}}{E_{m-U}} - 1\right) \qquad 2$$

$$\nu = \frac{E_{xm-U}}{E_{xm-B}}\left(\frac{E_{m-B}}{E_{m-U}} - 1\right) \qquad 3$$

where:

E_{xm-U} = modulus in cross-machine direction from a uniaxial test

E_{m-U} = modulus in machine direction from a uniaxial test

E_{xm-B} = modulus in cross-machine direction from a biaxial test

E_{m-B} = modulus in machine direction from a biaxial test

Use of Equations 2 or 3 is essentially a comparison of moduli between biaxial and uniaxial loading. This implies that the modulus values given in Equations 2 and 3 should be determined from specimens tested in the same device and should be determined at the same strain level, where this strain level should be relatively small. Currently, this requires that the biaxial device be used to test three specimens, two in uniaxial tension in each principal direction and one in biaxial tension. Further work is needed to determine if one specimen can be used for all three tests by applying relatively small loads in each successive test.

The in-plane shear modulus, G, is an elastic parameter needed for the input of elastic constants into a finite element response model for reinforced pavements. This parameter describes the in-plane stiffness of the geosynthetic to in-plane shearing forces. These forces may be caused by twisting or torque. Since most reinforcement materials are discontinuous within their plane, G is expected to be relatively small for all geosynthetics, however it is expected that stiff geogrids will have higher values than flexible materials such as woven geotextiles and geogrids.

For geogrids, the aperture stability modulus test (reference) is currently used to determine G according to a solution proposed by Perkins et al. (2004). In this solution, the aperture stability modulus (ASM) test was analyzed using elastic solutions to arrive at a simple relationship between G and ASM (Equation 4).

$$G = 7\,ASM \qquad 4$$

where G has units of kPa when ASM has units of N-mm/degree.

Geosynthetic-aggregate shear stress-displacement interaction for base-reinforcement design is also best described in terms of an interaction model of similar complexity to material models for the other pavement components. Since pavement response models are essentially resilient elastic models, shear interaction should also be described in terms of an elastic interface shear modulus. Like a resilient modulus for unbound aggregate, the interface shear modulus should be expected to be normal (bulk) stress and shear stress dependent.

Cuelho and Perkins (2005) have proposed a test that determines a geosynthetic-aggregate interface shear modulus as a function of normal stress con-

finement and applied shear stress. This test has recently become an ASTM standard (ASTM 7499, Measuring Geosynthetic-Soil Resilient Interface Shear Stiffness). The test is conducted as a cyclic pullout test on normal width specimens but where the embedment length is relatively short (2 apertures for geogrids). This is done to encourage uniform shear and displacement conditions across the specimen during cyclic loading.

The test is performed like a resilient modulus test on unbound aggregate in that a conditioning step is first applied by a series of cyclic loads under a given normal stress and constant cyclic pullout load amplitude. A number of load steps are then carried out under different combinations of constant normal stress and cycles of constant cyclic pullout load. For each load step, the interaction shear modulus, G_i, defined as the cyclic interface shear stress divided by the resilient interface shear displacement and having units of stress per distance or force per cubic distance, is determined as an average for the last 10 load cycles. This results in a single value of G_i for each combination of normal stress and cyclic shear stress.

Equation 5 has been proposed to relate G_i to normal stress, σ_i, and cyclic shear stress, τ_i. This equation is modeled after the equation for resilient modulus of unbound materials from NCHRP project 1-28a (NCHRP 2000). In this equation, P_a is taken as 101.3 kPa/m and is done to develop consistent units for G_i. The constants k_1, k_2, and k_3 are calibrated by a comparison of the equation to test results and are geosynthetic and aggregate dependent.

$$G_i = k_1 \cdot P_a \cdot \left(\frac{\sigma_i}{p_a}\right)^{k_2} \cdot \left(\frac{\tau_i}{p_a}+1\right)^{k_3} \qquad 5$$

A polyester geogrid and a coarse angular sand were used in a series of tests to evaluate G_i and the suitability of Equation 5 to describe results. In two tests, the applied maximum cyclic shear stress was held constant at 16 (Test 1) and 35 kPa (Test 2) for each test. The test was performed by applying 250 cycles of shear load at a series of confinements starting at 159 kPa and decreasing to 15.5 kPa. Measurements of G_i for each combination of shear stress and confining stress are shown in Figure 10, where it is seen that G_i increases with increasing confinement.

A second series of tests was performed by maintaining a constant confinement and increasing the applied maximum shear stress in a series of steps. This was repeated for three levels of confinement. Results for these two tests (Tests 3 and 4) are shown in Figure 11 where it is seen that G_i decreases with increasing cyclic shear stress.

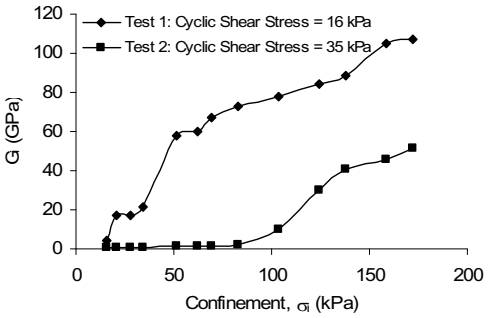

Figure 10. Interaction shear modulus, G_i, versus confinement for two levels of applied cyclic shear stress

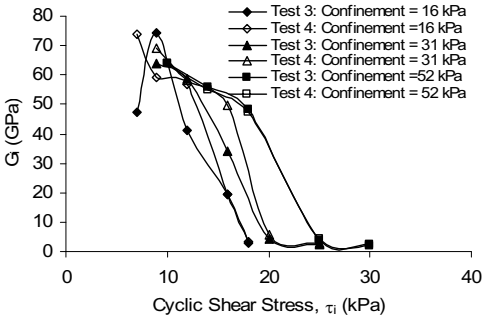

Figure 11. Interaction shear modulus, G_i, versus applied cyclic shear stress for three levels of confinement

Equation 5 was fit to the results presented in Figure 10 and Figure 11. The parameters k_1, k_2, and k_3 are resulting from this calibration are given in Table 3. A data fit measure (R^2) is shown, which provides a measure of fit between values predicted by Equation 5 and measurements from the test. It is seen that good values of R^2 are obtained, meaning Equation 5 is well suited for describing the data. In addition, the values of k_1, k_2, and k_3 are reasonably consistent between the different types of tests.

Table 3. Parameters k_1, k_2, and k_3 for cyclic pullout tests

Test	k_1	k_2	k_3	R^2
1	4.21E+07	0.707	-25.6	0.95
2	4.82E+07	0.754	-23.6	0.96
3	4.72E+07	0.622	-28.8	0.95
4	4.95E+07	0.632	-24.7	0.98

4 ASPHALT REINFORCEMENT

4.1 *Introduction*

Asphalt reinforcement has been practiced in various parts of the world for more than three decades. Successes have been reported on many occasions and

these have led to extensive use in certain types of pavement, for example those placed over very soft ground. Unfortunately there have also been a number of well publicized failures, most of which have been due to deficiencies during the construction process, and this has led to a certain amount of mistrust among highway engineers regarding what many consider to be a 'black art'.

Part of the reason for this is that asphalt reinforcement is most commonly used to combat reflective cracking, which is a notoriously difficult failure mode to predict, even without reinforcement, and existing methods of design do not generally include reflective cracking criteria. Reflective cracking is caused by repeated traffic loads, by one or more cycles of thermal contraction, or by a combination of these two mechanisms. The critical situations are shown in Figure 12: bending mode (Figure 12b); shearing mode (Figure 12a and Figure 12c); extension mode (Figure 12d). The role of a reinforcement system to combat reflective cracking depends mainly on its components. In outline it may be:

- To take up the localized stresses in the vicinity of cracks and, hence, reduce the stresses and strains in the bituminous material in the region of the crack tip. This is true reinforcement and geogrids of polymer, steel or glass fiber can fulfill this role, depending on their mechanical, durability and interaction properties.
- To provide a layer that is able to deform horizontally without breaking, in order to absorb the large movements taking place in the vicinity of cracks. This is the role of a SAMI (stress absorbing membrane interlayer), often a bitumen-impregnated non-woven geotextile. This role could also be described as "controlled debonding".
- To provide a waterproofing function and keep the road structure waterproof even after reappearance of the crack at the road surface. This can also be achieved using a bitumen-impregnated non-woven geotextile.

De Bondt (1999) indicated that an optimum solution to mitigate reflective crack propagation in asphalt overlays depends on the magnitude of horizontal and vertical movements of the underlying crack walls. Table 4, proposed by De Bondt, suggests different solutions based on qualitative levels of vertical and horizontal crack wall movement (low and high).

In summary, therefore, there is a need to:

a) quantify the effect of asphalt reinforcement on crack and rut development,
b) develop relevant laboratory tests for the assessment of reinforced asphalt,
c) model the effect of asphalt reinforcement by computer,
d) produce a usable design guide for reinforced asphalt roads.

This section of the paper will address the situation with regard to points a) and b).

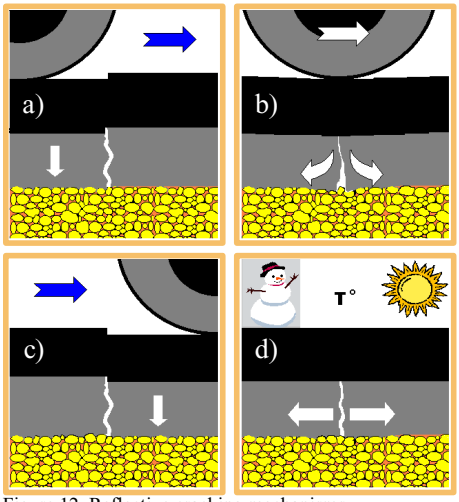

Figure 12. Reflective cracking mechanisms

Table 4. Recommendations De Bondt (1999)

Vertical crack movement	Horizontal crack movement	
	Low	High
Low	Thin overlay	Thin overlay + SAMI
High	Thin overlay + reinforcement	Thin overlay + modified binder + reinforcement

4.2 *A Review of Field Experience*

Over the past 30 years or so, a very large body of experience has been accumulated by those practitioners who have either experimented with reinforced asphalt or, in some cases, adopted it as standard practice. Unfortunately, much of this experience cannot be directly quantified or compared to the unreinforced alternative but it is, none the less, useful in giving an indication of the performance of the material.

Geotextiles are frequently used beneath a wearing course layer in strengthening overlays. This should probably not be referred to strictly as 'reinforcement', since the geotextile adds only limited strength or stiffness to the pavement. The interface created by the geotextile and the bituminous bond coat on which it is normally laid appears to form a crack barrier. Such treatments have been found to delay the development of reflective cracking from an underlying cracked or jointed pavement. For example, Karam (1993) reported the use of a geotextile beneath a 40-50mm wearing course on the RN91 in Belgium, a fatigued asphalt pavement. This treatment prevented cracking for six years, whereas the

adjacent unreinforced section had cracked 'severely'. He also reported two cases where semi-rigid pavements were treated in a similar way: the E42 in Belgium and the A64 in Spain. In both cases a control section had begun to fail after four years whereas the reinforced sections were still intact. Taniguchi and Ikeda (1998) presented results from the Japanese Accelerated Test Track where a similar system had been used beneath a 50mm wearing course in a semi-rigid pavement. Their results indicated that the rate of crack reflection was 30-50% of that in a control section. This result is also compatible with the findings of Laurent and Serfass (1993), who found that a geotextile beneath a 40mm layer in a flexible composite pavement resulted in about 50% of the number of cracks found in a control section. Walsh (1993) showed that a geotextile beneath a 50mm wearing course was also effective at delaying the occurrence of reflective cracks in an overlaid jointed concrete pavement. His results showed an approximately 50% reduction in cracking rate after three years. Karam (1993) also included an overlaid concrete pavement in his study, the RN427 in Belgium, this time with a geotextile beneath 80mm of wearing course and basecourse. This had showed very little cracking after seven years, whereas the control section had cracked badly at every joint. A wider description of the Belgian experience was given by Decoene (1993) who reported on 13 sites, mainly overlaid concrete, all but one of which were said to be performing well.

Geotextiles have also been used immediately beneath a surface dressing as reinforcement to a relatively light duty pavement. Perrier (1989) described such a process directly on an unbound base, and reported that it significantly enhanced the resistance of the pavement to deformation as well as surface break-up. Marchand (1993) also described experience with reinforced surface dressing on conventional pavements, and stated that the treatments were successful, both as crack retarders and also in maintaining the waterproofing function of the pavement.

The use of a geogrid represents a larger financial investment than a geotextile, implying that the return on that investment has to be correspondingly large. Herbst et al (1993) presented an interesting set of data from an experimental site in Austria, where the comparative benefits of geogrids and geotextiles could be directly assessed. The site was a concrete road which had already been overlaid with 110-130mm of asphalt, but which had subsequently cracked severely. Various treatments were carried out, involving the planing out of some or all of the asphalt and replacement by new materials. Whereas the section with 60mm of asphalt over polypropylene geogrid on a 30mm asphalt levelling course showed no cracking at all after nearly three years, 7% of the cracks on the equivalent geotextile reinforced section had appeared on the surface. Even on a 120mm unreinforced overlay section, 2% of cracks had appeared. However, where the geogrid was used without the 30mm levelling course, 6% of cracks had appeared. A corresponding section with steel grid (also without levelling course) allowed 27% of cracks to appear, and even more where no prior 'seating' treatment had been carried out.

Elsing and Sobolewski (1998) state that, in their experience, a factor of 4 on the life of a pavement as a result of the inclusion of a polyester geogrid is to be expected. The same geogrid was reported by Kassner (1989) to be particularly effective at a depth of 100mm over jointed concrete subject to severe temperature variations (-20 to +60°C). The reinforced pavement was performing well after 9 years, whereas the control section had cracked after 4 years. Schuster and Kuenzer (1989) described trials of both polyester and glass fibre geogrids laid under a wearing course layer over severe wheelpath cracking. After 2 years the control section had cracked whereas the reinforced sections were undamaged. Huhnholz (1996) presented direct evidence that a polymer geogrid gave a life enhancement factor of at least 3. On the A23 in Germany, a severely cracked and rutted pavement was planed out to a depth of 100mm and the grid fixed prior to 100mm of new asphalt being laid. After 7 years, no cracking had been reported where a previous similar unreinforced treatment had developed reflective cracking within two years.

An interestingly different use of geogrid reinforcement has been reported by Johansson and Nilsson (1998), where welded steel was successfully used beneath a wearing course to prevent cracking due to frost heave of the pavement.

It is clear from this brief review that many practitioners see significant benefit in using asphalt reinforcement across the range of products on the market. However, discrimination between products and between differing applications is difficult. With this proviso, the following points emerge:

a) One of the most effective uses for all the types of reinforcement is perceived as being for overlaying a deteriorated thin asphalt pavement
b) The use of a geotextile laid on a bituminous tack coat beneath an asphalt overlay may typically reduce the incidence of reflective cracking from an underlying cracked or jointed pavement layer by 50%.
c) Geogrid reinforcement is significantly more effective. It may typically increase the life of pavement by a factor of 4.

HVS full-scale accelerated pavement tests were also performed to examine the effect of a geotextile on the performance of a rehabilitated steep-sloped pavement structure (Korkiala-Tanttu et al. 2003b). The reinforced structures had around 25 - 50 % smaller rut depths than unreinforced reference struc-

tures. This corresponds to the lengthening of the service life by at least 50 %. The tests showed also that steel grid delayed fatigue to some extent.

Another HVS test with a reinforced asphalt layer were performed in the REFLEX project (Pihlajamäki et al.2002). According to the Reflex01 test with high pavement temperature (+40 °C) the service life of the steel reinforced structure was 30 - 45 % longer than the unreinforced structure with the same rut depth (Pihlajamäki et al. 2002). All the rutting occurred above the steel grid level and none below. Rutting occurred also in lower bituminous layers in unreinforced pavement.

4.3 *Traffic Simulation using Beam Tests*

The performance of a bitumen-impregnated geotextile system was clearly observed in a research program carried out at ITA (Aeronautical Institute of Technology, Brazil), where third-point flexure fatigue tests were conducted – see

Figure 13. Without a geotextile crack growth was straightforward; in the geotextile-reinforced case the crack grew until it reached the geotextile and was then redirected horizontally due to the controlled debonding between the geotextile and the asphalt.

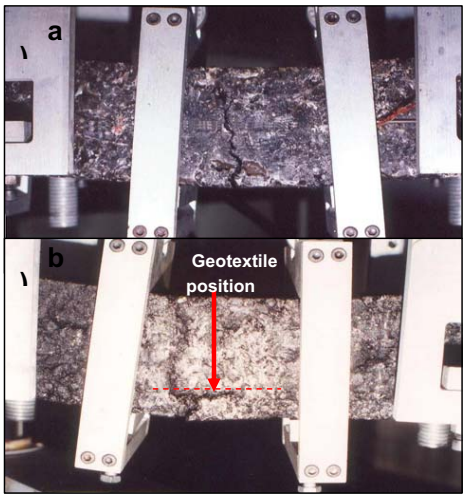

Figure 13. Dynamic flexure specimens: a) unreinforced; b) with geotextile (Montestruque 1996)

Research into polypropylene geogrid reinforcement of asphalt has been carried out at Nottingham since 1981 (e.g. Brown et al, 1985). Much of this work involved supported beam tests, where a crack in an underlying pavement was simulated by means of a split support over which the geogrid and the asphalt specimen were placed. Repeated vertical loading then led to the propagation of a crack upwards from the split in the support. The most important findings from these series of tests may be summarised as follows:

a) The geogrid did not affect the stiffness of the pavement to any significant degree.
b) A geogrid at the base of an asphalt layer resulted in a factor of up to 10 increase in fatigue life.
c) A grid at a shallow depth reduced rutting by a factor of about 3.
d) A grid at the bottom of an asphalt overlay provided a significant reduction in reflective cracking.

Parallel work was carried out to investigate the practicalities of paving over a reinforcing grid, since some installers had difficulty in ensuring that the grid remained in position during the paving process. Several different fixing systems were studied (Brown et al, 1989) and, as a result of this work and in recognition of installers' difficulties, the concept of a geotextile-geogrid composite was developed.

More recently Kim et al (1998) described beam tests which were very similar to those carried out at Nottingham. They investigated a number of crack inhibiting alternatives, including a glass fibre geogrid, which showed an improvement factor of between 4 and 8 on life (to an advanced state of cracking), depending on the asphalt mixture type involved.

Coppens and Wieringa (1993) also tested beams reinforced with glass fibre. However, their tests were conventional dynamic four point bending tests with the grid at a depth of 60mm in an 80mm deep beam. They did not test to cracking failure but rather allowed the beam to develop a permanent displacement under repeated vertical (downwards only) load. The presence of the relatively stiff glass fibre grid slowed down the development of the displacement by a factor of about 10.

Sanders (2001) described a test intended to simulate the situation in a pavement as realistically as possible, that is with a degree of continuity in support. The arrangement is shown in

Figure 14. A 10mm notch was cut in the base of the beam to ensure that the crack formed in a zone across which measurement devices were attached. An extensive series of tests was carried out at 20°C and 5Hz, on roller-compacted beams containing various reinforcement types.

Figure 14 gives the results in terms of the rate of crack growth, averaged for each of the specimen types tested.

Figure 14 shows that steel geogrid performed well, with a factor of enhancement on life of up to 3 over the unreinforced specimens. Polymer geogrid was almost as effective whereas glass fibre grids performed slightly less well, although the beam length used (400mm) was rather shorter that that

used by some other researchers and glass products are known to depend on a reasonable anchorage length either side of a developing crack. It is noticeable that a reduction in crack propagation rate due to the presence of reinforcement appeared even before the crack reached the level of the geogrid, and this is despite the reinforcement adding very little to the overall stiffness of the beam. It was suggested that this may be due to the geogrid effectively preventing localised permanent deformation.

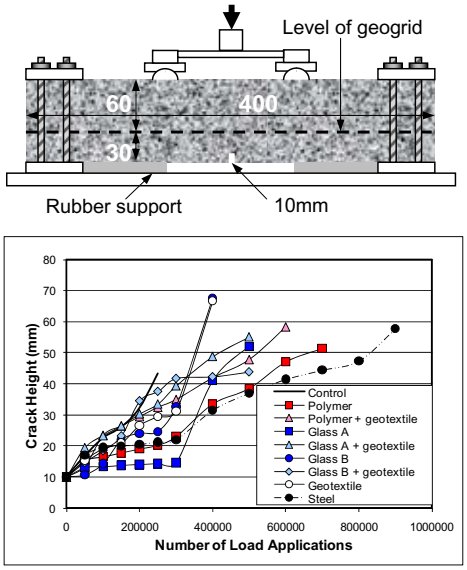

Figure 14. Partially supported beam tests (Sanders, 2001)

This was also clearly identified in dynamic fatigue tests on asphalt beams carried out at ITA, with and without polymer geogrids (Montestruque, 2002). The beams (46cm long x 7.5cm wide x 15cm high) were moulded in the laboratory, with an opening in the central lower part simulating a crack in an old asphalt layer. The geogrid was placed in the region of maximum stress concentration, over the opening tip. In beams without reinforcement the reflective crack appeared after a few cycles of loading and its growth was rapid and vertical (

Figure 15a). In reinforced beams the growth of the crack was interrupted and a quite different pattern of cracking was observed: micro-cracks initiated at random, associated with asphalt fatigue (

Figure 15b), but without any clear relation to a reflective cracking mechanism.

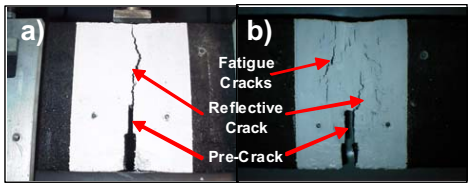

Figure 15. Dynamic fatigue specimens: a) unreinforced; b) geogrid reinforced (Montestruque, 2004)

4.4 *Pilot Scale Wheel Tracking Tests*

The Nottingham Pavement Test Facility (Brown and Brodrick, 1981) is an approximately half-scale loading facility which allows a single wheel load to traffic a pavement over a distance of around 5m. Sanders (2001) reports results from a pavement consisting of an 80mm asphalt layer placed onto a layer of 600mm by 600mm paving flags over sand bedding, granular sub-base and a low-stiffness clay subgrade. The layer of flags was intended to represent a severely cracked existing pavement. Six different sections were constructed as shown in Figure 16, the geogrid (where included) being placed at mid-depth in the asphalt. The wheel was applied on two different paths, each of which traversed two reinforced sections and a control section. The paving flags ensured that each reinforced section included at least two transverse joints. It was also decided to run a longitudinal joint at an offset of 100mm from the centre of the wheel path. The test was carried out initially at 20°C and then repeated at 14°C.

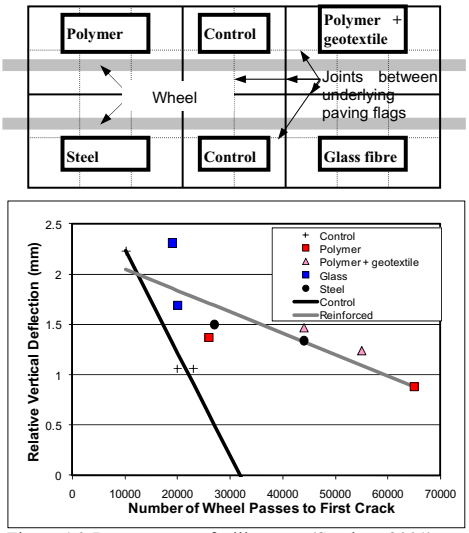

Figure 16. Pavement test facility tests (Sanders, 2001)

For each of the sections tested, the development of surface cracking was monitored throughout the test, as was the relative vertical movement between adjacent paving flags, at locations immediately adjacent to the wheel path. The results are plotted in Figure 16 as the number of wheel passes before the first appearance of reflective cracking on the surface against the measured relative vertical movement between flags, averaged over the whole test duration. This is a fairly crude simplification but it nevertheless indicates that there was a fundamental difference in behaviour between the reinforced and unreinforced cases, and that the enhancement in life in this case is by a factor of up to 2. Furthermore, this enhancement was achieved with the geogrid placed approximately at the neutral axis of the asphalt layer, implying that the mechanism applying was that of local inhibiting of crack formation rather than conventional reinforcement.

Wheel tracking tests continue to be used to explore the detailed mechanisms of reflective cracking and geogrid reinforcement, for example the use of LCPC equipment at the São Paulo University (USP), Polytechnic School - Transports Department - LTP, Brazil (Figure 17), and Nottingham, UK

Figure 17. Use of LCPC wheel tracking equipment for reflective crack investigation

4.5 *Thermally-Induced Cracking Tests*

Probably the best known early studies of thermally-induced cracking in asphalt overlays were carried out at the Belgian Road Research Centre. Francken (1990) describes a test that applied relatively slow load cycles by opening and closing the gap between two sections of concrete base over which a 70mm overlay had been laid. Francken and Vanelstraete (1993) present results from this equipment at -10°C, with a cycle time of 2 hours. Their results show that the presence of reinforcement fundamentally changed the stress strain behaviour of an asphalt overlay under the slow loading conditions applied and that, whereas a control specimen cracked after 3 cycles, in many cases the reinforced specimens survived >30 load cycles with no visible distress.

Brown et al (2001) simulated the opening and closing a crack in a cement-bound base directly using the equipment shown in

Figure 18. Specimens were placed and compacted in-situ, in two layers, the geogrid being placed on top of the first, 30mm thick, layer. A tack coat, spread at a rate of 0.5 litres/m^2, was used to bond the asphalt to the concrete base, which also had a textured surface. The end plates were removed after completion of the second layer of asphalt and then fixed back in place with an epoxy bond to the end of the asphalt, simulating the effect of a continuous pavement. Control of the motor was obtained via feedback from an LVDT which measured the relative movement of the two halves of concrete base. The motor was programmed to open the crack for a period of 4 hours and then to close it again for a further 4 hours. The test routine used was to carry out the first cycle with a crack opening of 0.5mm and then to increase this for each subsequent cycle, until failure of the specimen occurred. Tests were carried out at -5°C.

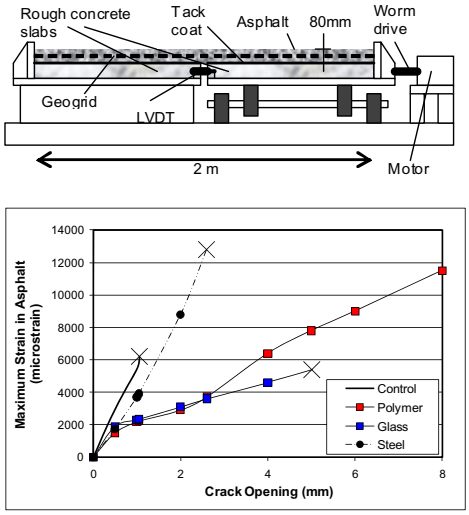

Figure 18. Thermal cracking test data (Brown et al, 2001)

Figure 18 shows the crack opening at which failure occurred, failure being taken as the occurrence of a severe full depth crack. It also shows the strain measured in the base of the asphalt directly above the gap in the concrete. As may be seen, the control specimen was the first to fail, at a maximum strain in the asphalt of about 6000 microstrain. The glass fibre reinforced specimen failed at a similar asphalt strain but at a much larger crack opening, because of its efficiency in spreading the strain laterally. The steel reinforced specimen withstood a greater asphalt strain (about 12,000 microstrain) before it failed, although the crack opening was relatively modest because the grid proved to be fairly inefficient at spreading strain longitudinally, due in part to the limited width of the specimen. The polymer geogrid reinforced specimen however withstood repeated

loading at a crack opening of 8mm and a measured asphalt strain of over 10,000 microstrain.

It is particularly interesting that the presence of certain types of geogrid reinforcement appears to alter the asphalt strain at failure, mirroring the way that tests under simulated traffic load appear to retard crack propagation at a given level of applied asphalt strain. The mechanism in both cases may be the inhibiting of localised permanent strains which would normally induce local crack formation.

4.6 *Summary*

Both experience in the field and research in the laboratory have revealed the fact that asphalt reinforcement can be effective. This applies to both geotextiles and geogrids, although each is best suited to particular pavement types. The mechanisms by which the reinforcement functions have been identified and include controlled debonding, modification of the stress and strain conditions in the asphalt, and also inhibiting of localised strain thereby avoiding the formation of single large cracks.

However, for confident analysis and design it is essential that these effects can be modelled properly and extrapolated from the accelerated case of a laboratory test to actual field performance. This subject will be reviewed in the following section.

5 MODELING AND DESIGN

5.1 *Base Reinforcement*

5.1.1 *Background*

International trends for the design of flexible pavements involves the use of mechanistic-empirical (M-E) methods, which requires the use of a mechanical response model to determine the stress-stain-displacement response of the pavement structure and empirical damage models to relate this response to long-term pavement performance defined in terms of permanent surface deformation and fatigue cracking. M-E methods are particularly suited for the evaluation of situations where new pavement materials are used and for which a significant historical data base of performance is not available. Given the complex nature of a geosynthetic reinforced flexible pavement and the introduction of a host of new variables associated with the reinforcement, a M-E procedure is ideally suited and even essential for providing a design method that is both generic and comprehensive.

In order to fit within the framework of modern M-E pavement design methods, the type of numerical response model should correspond as closely as possible to those in current pavement engineering practice. To date, the more sophisticated response models employed in traditional M-E methods have been necessary to show the effects of reinforcement. These response models have been finite element models employing non linear elastic models for the unbound materials. Finite element models are necessary in order to describe reinforcement layers using membrane elements and for describing interaction between the geosynthetic and the aggregate by appropriate contact models. Non linear elastic models for the unbound materials are necessary to show stress dependency and the effects of lateral restraint.

While these models are relatively sophisticated for the practice of pavement engineering, they are grossly inadequate in completely describing the complex problem of a reinforced pavement subject to many cycles of traffic load. Hence, it has been understood that in order to show the effects of lateral restraint when using design-grade response models, certain simplifications and approximations are necessary. The following sections describe a modeling approach that fits into the framework described above.

5.1.2 *Conventional Modeling Approach*

Modeling of base reinforced pavements has typically been performed within the context of finite element numerical models by which many studies have attempted to describe mechanisms of reinforcement. These models have most commonly been developed by direct inclusion of structural elements for the reinforcement sheet and contact surfaces between the reinforcement and surrounding materials. Models established in this fashion have historically shown a gross under prediction of pavement performance and corresponding benefit from the reinforcement, which is due to the inability of a simple static, single load cycle response model analysis to show the effect of lateral confinement due to base compaction and repeated traffic loading.

As an example, Perkins et al. (2005) developed a conventional finite element model of a reinforced pavement by following guidelines established in NCHRP Project 1-37a (NCHRP 2003) for the pavement components not associated with the reinforcement. The commercial program ABAQUS was used for these models. The model was a two dimensional axisymmetric model using 4 noded quadratic elements for the asphalt concrete, base aggregate and subgrade layers and with boundary conditions simulating box test sections reported by Perkins (1999) to which the model was compared. The thickness of the asphalt concrete, base aggregate and subgrade layers was set to match the conditions of one reinforced test section with thickness of 77, 300 and 1045 mm, respectively. A uniform pressure of 550 kPa was applied over a radius of 152.4 mm on top of the asphalt surface for pavement load and matched conditions present in the comparison test section.

An isotropic linear elastic model was used for the asphalt concrete layer. An isotropic non-linear elastic model was used for the base aggregate and subgrade materials. The model describes the resilient modulus (M_R) as a function of bulk stress (θ) and deviatoric stress (τ_{oct}) (Equation 6), where p_a is atmospheric pressure (100 kPa) and k_1, k_2, k_3 are material properties determined from resilient modulus tests.

$$M_R = p_a k_1 \left(\frac{\theta}{p_a} \right)^{k_2} \left(\frac{\tau_{oct}}{p_a} + 1 \right)^{k_3} \qquad 6$$

Reinforcement was modeled by including a material layer consisting of a thin sheet composed of 2-node membrane elements. Membrane elements have the ability to carry loads in tension but have no bending stiffness or ability to carry load in compression. An isotropic linear elastic model having input parameters of elastic modulus and Poisson's ratio was used for the reinforcement material. An equation was developed (Perkins & Eiksund 2005) to determine the isotropic linear elastic modulus and Poisson's ratio from actual direction dependent orthotropic properties (elastic modulus in each principal direction, in-plane Poisson's ratio and in-plane shear modulus). The tests described in Section 3.3 were used to determine these properties for the small-strain/displacement conditions present in pavements. For the geogrid material contained in the comparison test section, elastic modulus and Poisson's ratio were 426 MPa and 0.25 respectively.

The upper and lower surfaces of the reinforcement were set up to be contact surfaces. Shear interaction along each contact surface was described in terms of a Coulomb friction model, which allowed for the specification of an interface shear stiffness, which in turn was determined from cyclic pullout tests.

Pavement load was applied to the reinforced model described above. An example analysis was performed with a reinforced model set up according to the steps described above and compared to an identical model without reinforcement. From these models, the vertical strain along the model centerline axis in all pavement layers was extracted and used in empirical damage models for rutting to determine pavement permanent surface deformation as a function of applied load cycles with results shown in Figure 19.

The reinforced model showed only a modest (8.4 %) increase in the number of traffic passes carried at a surface deformation of 25 mm (53,850 vs. 58,400 traffic passes). For this test section with this particular reinforcement product, the reinforced test section was seen to carry approximately 600,000 load passes necessary to reach 25 mm of surface deformation. These results show the inability of this simple and conventional method for modeling reinforcement and points to the need for additional considerations for reinforced response models that account for the effect of lateral restraint created during compaction and traffic loading of the pavement.

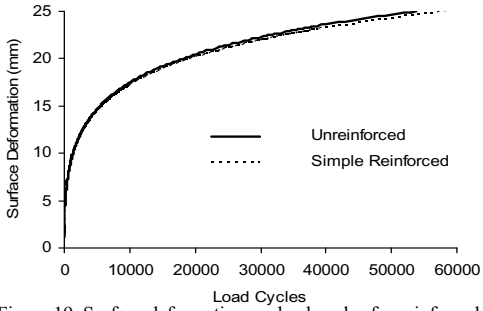

Figure 19. Surface deformation vs. load cycles for reinforced model and comparative unreinforced model using simple reinforcement modeling (Perkins et al. 2005).

5.1.3 *Response Model Modules*

Response model modules were developed that simulate certain construction and traffic loading effects that the reinforcement has on the pavement system. The non-linear elastic material model used for the base aggregate and subgrade imposes certain limitations in rigorously modeling the effects of the reinforcement. This relatively simple constitutive model is insufficient for exactly describing the full sequential process of construction followed by the application of many repetitions of vehicular traffic. Since the material model for the base aggregate shows improved performance through an increased elastic modulus arising from an increase in mean stress, the response model modules were developed to yield an increase in aggregate confinement during compaction and traffic loading. Hence, the response model modules show an increase in horizontal stress in the aggregate, which has a reasonable physical basis as supported by research described in Section 3.1, yet the modeling methods for doing so are partially physically artificial but necessary given the limitations of the material models used.

The response model modules include a model describing effects during compaction and three response models used in succession and in an iterative manner to describe the effects of reinforcement during traffic loading. Figure 20 provides a flow chart of these response models. The Compaction and Traffic I response model modules are analyzed once for a given pavement cross section. The Traffic II and III models are analyzed a number of times to describe pavement response during different periods of the pavement life as permanent strain is developed in the reinforcement.

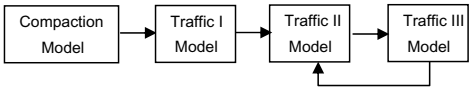

Figure 20. Flow chart of response model modules

5.1.4 *Compaction Model*

Material presented in Section 3.1 showed that locked-in horizontal stresses exist in aggregate layers compacted on top of a geosynthetic. From a response modeling perspective, greater lateral stresses at the beginning of an analysis will mean that modulus of the material will be initially higher when non-linear stress-dependent elastic material models are used.

The principal effect of the reinforcement layer during compaction is to limit lateral movement of the aggregate as compaction tends to compress and shove material vertically and laterally. On a local level, restraint is provided by aggregate interacting with and transferring load to the reinforcement. As compaction equipment is worked around on the aggregate layer, aggregate never assumes a predominant direction of motion, meaning that the creation of tensile strains in the reinforcement may be negated and reversed when equipment operates in another location. The effect of this random process is to leave the aggregate with possibly a greater density but more importantly with locked-in horizontal stresses and the geosynthetic in a relatively strain-free state. As such, the process should not be viewed as a reinforcement pretensioning effect, which experimentally has not been shown to be effective. The tensile modulus of the reinforcement is, however, important in this process in that it will contribute to the reduction of lateral movement of the aggregate during each pass of a piece of compaction equipment and will contribute to the build up of locked-in horizontal stresses. In addition, the contact properties between the aggregate and the reinforcement are of importance with interfaces showing less shear stiffness leading to lower values of locked-in horizontal stresses.

A simple procedure was sought to model this process within the context of a finite element pavement response model. Exact replication of this random and complex process is extremely difficult and unwarranted. The procedure developed involves assigning thermal contractive properties to the reinforcement sheet and creating shrinkage of the material by applying a temperature decrease. This produces relative motion between the geosynthetic and the aggregate and essentially models in reverse and in a simplified way the complex effect of aggregate being shoved laterally back and forth during compaction.

Once the temperature decrease has been applied, horizontal stresses at the element centroid are extracted from the model for a column of elements in the base along the model centerline. These horizontal stresses, along with the geostatic vertical stresses due to material self-weight, are then used as the initial stresses for the entire base layer in a subsequent reinforced response model (i.e. the Traffic I model). These steps provide a means of describing the locked-in horizontal stresses in the aggregate due to relative motion between the aggregate and the reinforcement during compaction.

To illustrate the effect of this step, a third analysis was performed by taking the reinforced model described previously and using the initial stress state for the base from the compaction model described above before applying pavement load. Figure 21 shows the results from this analysis as compared to the previous two analyses. The reinforced model with the compaction induced stresses results in 23 % more traffic passes necessary to reach 25 mm of surface deformation. While this is an improvement over the simple reinforced model, the result is still far below the benefit seen in this test section, indicating that additional considerations are needed.

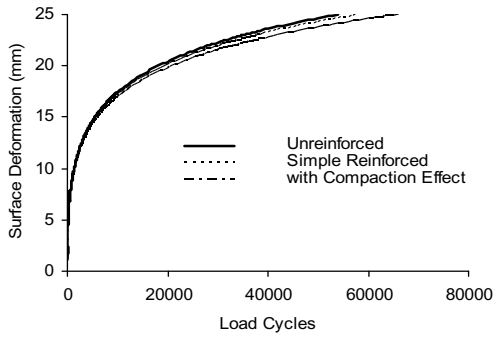

Figure 21. Surface deformation vs. load cycles for reinforced model with compaction model induced initial stresses (Perkins et al. 2005).

5.1.5 *Traffic I Model*

In addition to an increased horizontal stress due to compaction of aggregate on top of a layer of reinforcement, lateral confinement of the aggregate base layer develops during vehicular loading of the roadway. Additional lateral confinement is due to the development of interface shear stress between the aggregate and the reinforcement, which in turn transfers load to the reinforcement. As a cycle of traffic load is applied, there is both a transient or cyclic shear stress and a residual shear stress that exists when the traffic load is removed. The residual interface shear stress continues to grow as repeated traffic loads are applied, meaning that the lateral confinement of the aggregate base layer becomes greater with increasing traffic load repetitions. The Traffic I response model module is used to provide data for the transient interface shear stress distribu-

tion between the reinforcement and the surrounding materials.

Experimental data from test sections where geosynthetics have been instrumented shows the development of permanent radial strain in the reinforcement with traffic load applications. Experimental data and theoretical considerations with simplifying approximations have been made to show the equality between the ratio of permanent to resilient strain in the reinforcement to the ratio of residual to transient shear stress on the reinforcement-aggregate interface (Perkins and Svanø 2006). This leads to Equations 7 and 8 describing the residual shear stress on the interface as a function of traffic passes.

$$\tau_r = \tau_t \frac{\varepsilon_p}{\varepsilon_r} \quad 7$$

$$\log\left(\frac{\varepsilon_p}{\varepsilon_r}\right) = \log(A) + B\log\left(\frac{N}{N_{25\,mm}}\right) \quad 8$$

where:
τ_r: residual shear stress on interface
τ_t: transient shear stress on interface
ε_p: permanent strain in the reinforcement
ε_r: resilient strain in the reinforcement
$N/N_{25\ mm}$: ratio of actual traffic passes to passes necessary for 25 mm permanent deformation
A, B: Interface shear stress growth parameters

Parameters A and B are currently calibrated from geosynthetic strain measurements in test sections. The Traffic I module provides a means of determining the transient interface shear stress (τ_t) for use in Equation 7. From this model, the interface shear stresses are extracted when full pavement load is applied. This interface shear stress distribution is taken as the values for τ_t as a function of model radius.

The resulting shear stress distribution is then scaled by selected values of $\varepsilon_p/\varepsilon_r$ leading to new shear stress distribution curves representing different periods in the life of the pavement. Equivalent nodal forces are then calculated by distributing the shear stresses over the contributory area of each node and used in the subsequent Traffic II model to examine the effects of this shear stress distribution.

5.1.6 *Traffic II Model*

The Traffic II response model module gives the elevated horizontal stresses in the base due to compaction effects and for the additional locked in stresses due to the increasing tensile strains in the reinforcement with increasing traffic. This is accomplished by applying the nodal forces due to the residual interface shear stresses for a particular pavement life period from the Traffic I model to an unreinforced model having an identical cross-section and pavement layer properties.

The Traffic II model starts with an initial state of stress that comes from that determined in the Compaction model. Nodal forces calculated from the Traffic I model analysis are then applied to nodes in the base at the same level where the reinforcement was present. Once these nodal forces have been applied, the horizontal stresses at element centroids for the column of base aggregate elements along the model centerline are extracted. These horizontal stresses along with the geostatic vertical stresses are then taken as initial stresses in a subsequent and final response model (i.e. Traffic III module).

The analysis using the Traffic II model is repeated for the number of $\varepsilon_p/\varepsilon_r$ ratios selected to determine equivalent nodal forces. Thus the Traffic II analysis provides a means of assessing the effect of residual interface shear stresses on lateral stresses developed in the base aggregate layer for different periods in the life of the pavement within the context of a finite element response model.

5.1.7 *Traffic III Model*

The Traffic III model uses the same pavement response model as the Traffic I model but uses the horizontal stresses determined from the Traffic II model along with the geostatic vertical stresses as initial stresses. This model is run for the same number of Traffic II models evaluated. From each model, the distribution of vertical strain versus depth along the model centerline is extracted and used in conjunction with the damage models for permanent deformation to determine permanent surface deformation for the load cycles that apply to the period for which the $\varepsilon_p/\varepsilon_r$ ratios apply.

For each data set of vertical resilient strain versus depth, the damage models for permanent deformation are used to determine a curve of permanent surface deformation versus traffic load applications. This curve is taken to apply to the load cycles ranging from the previous $\varepsilon_p/\varepsilon_r$ ratio to the current $\varepsilon_p/\varepsilon_r$ ratio. A cumulative surface deformation curve is then computed by taking deformation that occurs for each period and accumulating it over the number of analysis periods. Figure 22 shows the resulting curve as compared to the previous analyses where it is seen that the model with compaction and traffic effects offers considerable improvement.

5.1.8 *Other Considerations*

The above procedure resulted in a significant improvement in predicting reinforced pavement performance as compared to conventional procedures. Additional work involving large-scale cyclic triaxial testing of reinforced aggregate (Eiksund et al. 2004) has shown that reinforcement reduces the development of vertical permanent strain under repetitive loading. These tests were used to develop damage laws for the permanent strain for reinforced aggregate. This work also showed that the modified damage law should be only applied for a zone of aggregate adjacent to the reinforcement of 150 mm in

thickness or where the degree of stress mobilization exceeds a threshold value corresponding to an angle of 30 degrees. When these equations and considerations are applied to the aggregate in the test section modeled in this paper, the resulting predicted surface deformation vs load cycle curve is shown in Figure 23. The measured response from the test section is also shown on this figure. This figure shows a reasonable correspondence between the mechanistic-empirical prediction and results physically measured from a test section.

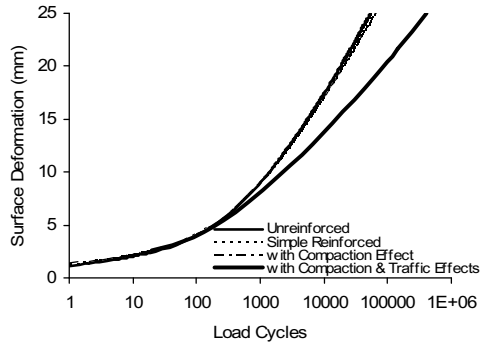

Figure 22. Surface deformation vs. load cycles for reinforced model with compaction and traffic induced initial stresses (Perkins et al. 2005).

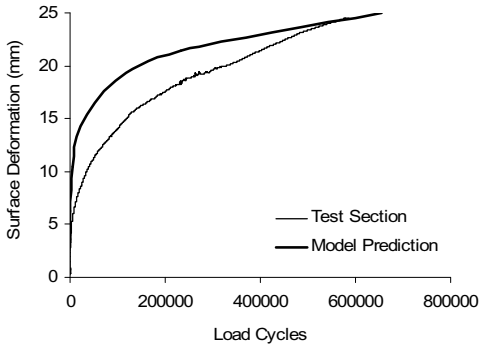

Figure 23. Permanent surface deformation vs load cycles for procedure including reduced permanent strain in the reinforced base aggregate

5.2 *Subgrade Stabilization*

Recent work has applied the M-E method described in Section 5.1 to reinforced unpaved roads (Perkins et al. 2008 and Christopher et al. 2009). The M-E method was compared to results from unpaved box test sections constructed on a micaceous silt subgrade having a CBR of 1.0. The model was calibrated against unreinforced unpaved test sections and then analyzed for reinforced sections containing a woven geotextile.

Analysis of the reinforced test section showed an underprediction of rutting performance by the model. This was attributed to the effect of the reinforcement on the development of excess pore water pressure in the subgrade. As discussed in Section 2, excess pore water pressure build-up with repetitive pavement loading is significant, particularly in unpaved roads where the dynamic stresses imposed on the subgrade are substantial. For the unpaved test sections discussed in Perkins et al. (2008), the excess pore water pressure in the unreinforced test section was approximately 21 kPa while in the reinforced test section it was 7 kPa. Development of pore pressure reduces the effective stress in the subgrade and thereby reduces the subgrade stiffness and strength. The reduction of stiffness and strength has a dramatic impact on the rutting performance of the roadway.

Christopher et al. (2009) presented a method to account for the influence of excess pore water pressure on strength and stiffness of the roadway subgrade. The method relies upon the use of well established soil mechanics principles to relate the undrained shear strength of a clay subgrade (S_{uf}) to the initial undrained shear strength (S_{ui}) and the excess pore water pressure (u_e) (Equation 9). The method assumes that the clay subgrade can be described as a normally consolidated clay with an effective strength friction angle (ϕ) and an effective strength cohesion of zero. Skempton's pore water pressure parameter A is used to relate excess pore water pressure to induced normal stresses. Equation 9 reduces to Equation 10 when ϕ is taken as 30° and A is taken as 0.2.

$$S_{uf} = S_{ui} - \frac{u_e}{\frac{2}{\tan^2(45+\phi/2)-1} + 2A} \qquad 9$$

$$S_{uf} = S_{ui} - \frac{u_e}{1.4} \qquad 10$$

The M-E method presented in Section 5.1 was amended to account for the influence of excess pore water pressure by using a reduced elastic modulus for the subgrade in the finite element response model. The reduction of elastic modulus from the initial, as-constructed condition, was assumed to be proportional to the reduction of subgrade undrained shear strength from the initial to the final condition as given in Equation 10. The excess pore water pressure observed in the test sections was used in Equation 10 when matching the model to results from test sections.

There is an insufficient understanding of how pore pressure generation in weak subgrades subject to traffic loading is dependent on subgrade type, wheel load configuration, aggregate thickness and

reinforcement. Presently, the effect of excess pore water pressure as accounted for by Equations 9 and 10 is possible only by knowing the magnitude of u_e in an unreinforced cross section and the percentage reduction in u_e for a reinforced section. This requires information from test sections, which lacks generality for purposes of design. Future research should focus on methods to predict cyclic pore water pressure generation for conditions pertinent to unpaved roads.

Kanerva-Lehto (2009) has presented a method for dimensioning a steel grid reinforcement for frost heave cracks repairing. In the method the road structure is seen as a cantilever.

5.3 *Modeling Reinforcement Influence*

Reinforcement in asphalt is primarily intended to inhibit crack development and the influence of reinforcement therefore has to be set against the background of an asphalt fatigue cracking law. It is not the purpose of this paper to constrain the choice of fatigue law. Fracture mechanics and damage mechanics represent alternative approaches at two ends of a spectrum of possibilities. The CAPA finite element package (Scarpas et al, 1993) for example, developed at Delft University of Technology, is a program that is used to predict the effects of geogrid reinforcement in practice, incorporates fracture mechanics in its asphalt model. On the other hand, the pattern of numerous small cracks induced by reinforcement, as illustrated in Figure 15, suggest that damage mechanics is an attractive alternative.

However the critical issue in modelling the effect of reinforcement is to determine the way in which the reinforcement affects crack propagation (or damage progression). In general there are two effects, paralleling those operating in granular media, namely:

1. Load carried by the reinforcing strands and/or controlled debonding beneath a geotextile layer changes the stresses and strains applying at a crack tip;
2. The presence of reinforcement inhibits the local straining required for crack (or damage) progression.

The following subsections will discuss these issues in turn.

5.3.1 *Induced Stress Change – Stress Relief*

A low-stiffness-modulus bitumen-impregnated geotextile acts as a stress relieving interlayer in an overlay system. Since it is a low modulus system, it does not affect the opening and closing movement of the cracks, but due to its capability of retaining a certain amount of tack coat, it becomes a thick viscoelastic layer that dissipates the stresses in the crack tip and deviates the direction of propagation, as seen experimentally in beam tests in Figure 13.

Figure 24 illustrates a finite element analysis of the beam test arrangement with and without a geotextile interlayer and demonstrates the way that the interlayer changes the stress distribution, reducing the magnitude of maximum tensile stress.

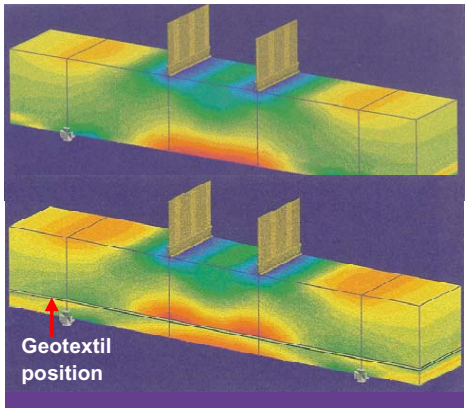

Figure 24.. Finite element model of beams with and without a geotextile layer (Montewtruque 1996)

5.3.2 *Induced Stress Change – Crack Stitching*

In an unreinforced beam a crack can simply open up as it grows. A key effect of any reinforcement present is to hold the two sides of the crack together, reducing the stresses and strains in the region of the crack tip and therefore reducing the crack propagation rate. Finite element simulations were performed to interpret the results obtained during the dynamic fatigue testing shown in Figure 15, based on the global energy principle and using the node release technique in order to simulate the crack propagation observed in the laboratory. The analysis (Figure 25) showed that, at the initial stage, the crack tip was the region of maximum tensile stresses but that there was a reduction in these stresses due to the inclusion of the geogrid. As the nodes were released, simulating crack propagation, different behavior was noticed in beams with and without geogrid. In simulations without geogrid the maximum tensile stress region remained at the crack tip, explaining the rapid propagation observed in the laboratory. In tests with a geogrid, as the nodes were released the tensile stresses decreased progressively at the crack tip and increased in the geogrid region. At a certain point the tensile stress level at crack tip was small enough not to allow propagation, again matching observations made in the laboratory.

Numerical simulations such as these allow improved understanding of the effect of reinforcement on crack propagation. Nevertheless it is usual to simplify the actual effect of individual reinforcing strands with unreinforced apertures between them. It is also necessary to simplify crack propagation in

some way by means of a crack growth or damage progression law.

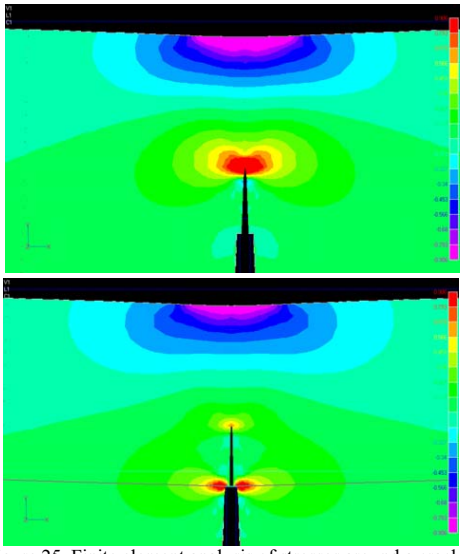

Figure 25. Finite element analysis of stresses around a crack with and without geogrid (Montestruque, 2004)

5.3.3 *Inhibiting Local Straining*

It was observed in Section 4 (Figure 16) of this paper that changes to stress distribution appeared to be insufficient to explain some of the experimental data, for example the increase in time before reflective cracking observed in the University of Nottingham pavement test facility even when the reinforcement was placed approximately on the neutral axis of the asphalt layer. This phenomenon may be explained in terms of inhibiting of permanent strain local to the geogrid due to its elastic recovery properties, since even microcrack formation implies the development of a finite permanent strain. Brown et al (2001) proposed that the most appropriate way to take this effect into account was to apply a 'fatigue factor', reducing crack propagation rate over a zone of influence, the factor depending on the efficiency with which the geogrid carried out this function. Using a strain-related crack propagation law ($dc/dN = A\ \varepsilon^n$) they determined on the evidence of the beam tests illustrated in Figure 14 that a factor of about 0.25 applied to the most effective geogrid types. However the zone of influence proposed was only around 30mm either side of the reinforcement. Furthermore it was observed that where a geotextile was incorporated into the reinforcement system this fatigue cracking reduction factor no longer applied to the material adjacent to the geotextile, i.e. it depended on interlock with the reinforcing strands of the geogrid.

In many respects this approach directly parallels the suggestion made in Section 5.1 (Eiksund et al, 2004) that reinforcement of granular materials can also be modelled using a modified damage law over a certain zone of influence.

5.3.4 *Reflective Cracking Due to Traffic*

The goal of all pavement modelling is to successfully simulate actual highway performance, something for which there is as yet no agreed procedure with regard to reflective cracking. This section will describe one possible approach and its application to reinforced asphalt, but it is acknowledged that many others exist. Figure 26 is a two-dimensional representation of the passage of a wheel over an overlay to a cracked or jointed layer beneath. In the procedure described by Thom (2003) the asphalt overlay is allowed to detach from the underlying material, bending as required in order to support the load. The curvature of the asphalt depends on all the material moduli and thicknesses, the load, the degree of load transfer across the cracks and the crack spacing. If a crack has already started to develop in the asphalt overlay then a correction to its effective modulus is made.

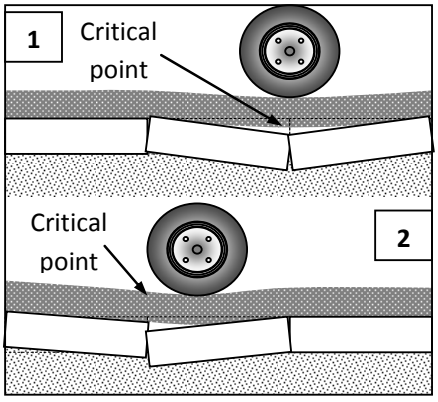

Figure 26. Simplified analysis of reflective cracking

This analysis is simple and determinate and so is suited to an iterative procedure. It allows the strain in the asphalt in the region of a crack tip to be calculated and this is related to crack propagation rate. It also allows both top-down and bottom-up cracking to be modelled, once corrections have been made for additional straining within the overlay material beneath the load and to convert to the real three-dimensional case.

The effect of geogrid reinforcement was included both by considering the stress redistribution caused after the crack had propagated past the geogrid and also by incorporating a factor on crack propagation

rate as described in the previous section. Figure 27 shows selected predictions using this approach for an overlayed cracked asphalt pavement, assuming an effective reinforcement layer (factor of 0.25 on crack propagation rate).

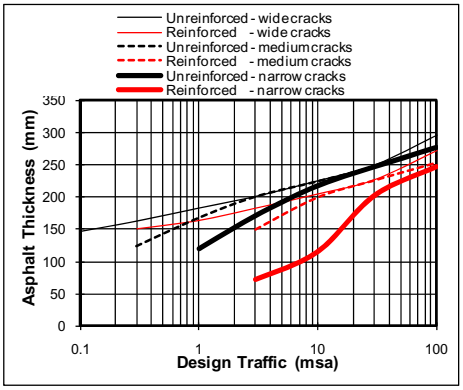

Figure 27. Designs generated for a reinforced asphalt overlay to a cracked asphalt pavement

If this approach is to be trusted then it is evident that the benefit of reinforcement is heavily dependent on the pavement being overlaid. In this case maximum benefit is obtained over a medium-traffic pavement with narrow (and therefore close-spaced) cracks.

5.3.5 *Reflective Cracking Due to Temperature*

This situation is less complex than that due to traffic load in that it is essentially a two-dimensional problem. Figure 28 illustrates the type of analysis required and this can be by means of either simple determinate approximation or a finite element computation. It is not difficult to predict the temperature fluctuation within the pavement layers during a given 24-hour period and the consequent thermal contraction. As is well understood, this contraction generates tensile stress, part of which can be carried by reinforcing grid if present. Nevertheless it is still necessary to calibrate any prediction against experience since the detailed influence of individual reinforcing strands on the onset of cracking is complex and also because temperature regimes vary throughout the year.

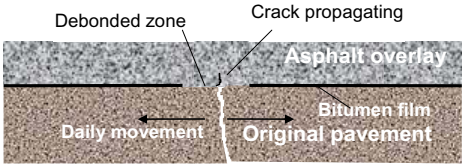

Figure 28. The system to be modelled with respect to temperature effects

By way of example, Thom (2003) presents calculations for overlaid jointed concrete pavements that indicate a reduction in overlay thickness from 18cm, the suggested 'safe' value for major UK highways, to 12.5cm when geogrid reinforcement is included, a significant saving.

Clearly the reality of design is that both thermally induced and traffic induced effects have to be considered. Computationally it is quite possible to consider both together; but on the other hand crack propagation develops quite differently under slow loading compared to rapid loading, and it may therefore be prudent to consider them separately. In general it is found, both through modelling and from experience, that geogrid reinforcement is highly effective against thermally induced cracking but that this benefit can only be realised in cases where there is sufficient load transfer across cracks in the original pavement.

6 SUMMARY AND CONCLUSION

This paper has presented a review and recent results of research pertinent to various applications of geosynthetics for reinforcement of roadway pavements. The applications of subgrade stabilization, base reinforcement and asphalt reinforcement have been discussed. Particular emphasis was placed on the mechanisms in operation for each application, a demonstration of pavement performance and benefit from the reinforcement layer in full-scale tests, and geosynthetic material properties and tests pertinent to the application. A discussion of performance tests, such as beam tests, wheel tracking tests and cracking tests, for asphalt reinforcement was presented. Recent activities in the area of numerical modeling and design of pavements were discussed. Models that fall within the category of mechanistic-empirical methods were given special attention.

REFERENCES

AASHTO 2006. Standard Specifications for Geotextiles - M 288, *Standard Specifications for Transportation Materials and Methods of Sampling and Testing*, 26th Edition, American Association of State Transportation and Highway Officials, Washington, D.C.

AASHTO 2001. Recommended Practice for Geosynthetic reinforcement of Aggregate Base Course of Flexible Pavement Structures. *AASHTO Designation 46-01*, AASHTO, Washington DC.

Al-Qadi, I. L. & Appea, A. K. 2003. *Eight-Year Field Performance of A Secondary Road Incorporating Geosynthetics at the Subgrade-Base Interface*, Transportation Research Board-82nd Annual Meeting, January 12-16, Washington, D.C.

Al-Qadi, I. L., Brandon, T. L., Valentine, R. J., Lacina, B. A., & Smith, T. E. 1994. Laboratory Evaluation of Geosynthetic-Reinforced Pavement Sections,

Transportation Research Record 1439, TRB, National Research Council, Washington, D. C., pp. 25-31.

Austin, D. N. & Coleman, D. M. 1993. A Field Evaluation of Geosynthetic-Reinforced Haul Roads Over Soft Foundation Soils, *Proceedings of the Conference Geosynthetics 93*', Vancouver, Canada, pp. 65-80.

Bender, D.A. & Barenberg, E.J. 1978. Design and Behavior of Soil-Fabric-Aggregate Systems, *Transportation Research Record 671*, TRB, National Research Council, Washington, DC, USA, pp. 64-75.

Berg, R.R, Christopher, B.R. & Perkins, S.W. 2000. *Geosynthetic Reinforcement of the Aggregate Base/Subbase Courses of Pavement Structures, GMA White Paper II*, Geosynthetic Materials Association, Roseville, Minnesota, USA, 176 p.

Barksdale, R.D. & Alba, J.L. 1993. *Laboratory Determination of Resilient Modulus for Flexible Pavement Design*. Interim Report No. 2, NCHRP, TRB, National Research Council, Washington DC, USA.

Barksdale, R.D., Brown, S.F. & Chan, F. 1989. *Potential Benefits of Geosynthetics in Flexible Pavement Systems*, National Cooperative Highway Research Program Report 315, Transportation Research Board, Washington, D.C., 56 p.

Black, P.J. & Holtz, R.D. 1997. *Performance of Geotextile Separators: Bucoda Test Site — Phase II*, Washington State Department of Transportation Report WA-RD 440.1, 210 p.

Brandl, H., Koph, F. & Adam, D. 2005. Continuous Compaction Control (CCC) with Differently Excited Rollers. In: Schriftenreihe der Strassenforschung Heft 553, Forschungsvorhaben Nr. 3.176, Bundesministerium für Verkehr, Innovation und Technologie, Wien.

Brown, S.F., & Brodrick, B.V. 1981. The Nottingham pavement test facility. *Transportation Research Record*, 810, pp. 67-72.

Brown, S.F., Brunton, J.M., & Armitage, R.J. 1989. Grid reinforced overlays. *Proc. 1st Int. RILEM Conf. Reflective Cracking in Pavements*, Liege, pp. 63-70.

Brown, S.F., Brunton, J.M., Hughes, D.A.B., & Brodrick, B.V. 1985. Polymer grid reinforcement of asphalt. *Proc. Association of Asphalt Paving Technologists*, 54, pp. 18-41.

Brown, S.F., Thom, N.H., & Sanders, P.J. 2001. A study of grid reinforced asphalt to combat reflection cracking. *Asphalt Paving Technology*, 70, pp. 543-571.

Cai, M., & Horii, H. 1994. A simple homogenization method for cracked solids. *Damage Mechanics in Composites*, pp. 191-199.

Christopher, B.R., Perkins, S.W., Lacina, B.A. and Marr, W.A. 2009. Pore Water Pressure Influence on Geosynthetic Stabilized Subgrade Performance, *Proceedings of the Conference Geosynthetics 2009*, Salt Lake City, Utah, USA.

Christopher, B.R. & Lacina, B. 2008. Roadway Subgrade Stabilization Study, *Proceedings of the Conference GeoAmericas 2008*, Cancun, Mexico, pp. 1013 -1021.

Christopher, B.R. and Perkins, S.W. 2008. Full scale testing of geogrids to evaluate junction strength requirements for reinforced roadway base design, *Proceedings of the Fourth European Geosynthetics Conference*, Edinburgh, United Kingdom, International Geosynthetics Society.

Christopher, B.R., Berg, R.R & Perkins, S.W. 2001. *Geosynthetic Reinforcement in Roadway Sections*. NCHRP Project 20-7, Task 112, TRB, National Research Council, Washington DC.

Collin, J.G., Kinney, T.C. & Fu, X. 1996. Full Scale Highway Load Test of Flexible Pavement Systems with Geogrid Reinforced Base Courses, *Geosynthetics International*, Vol. 3(4), pp. 537-549.

Coppens, M.H.M., & Wieringa, P.A. 1993. Dynamic testing of glass fibre grid reinforced asphalt. *Proc. 2nd Int. RILEM Conf. Reflective Cracking in Pavements*, Liege, pp. 200-205.

COST-348 WG1 2004: *Reinforcement of pavements with steel meshes and geosynthetics. (REIPAS) Assessment of benefits and goals for different reinforcement applications. Draft Report of WG 1*, chaired by Chris Jenner.

Cuelho, E.V. & Perkins, S.W. 2005. Resilient Interface Shear Modulus from Short-Strip, Cyclic Pullout Tests. *Proceedings of the Conference GeoFrontiers, Geotechnical Special Publication 140, Slopes and Retaining Structures under Seismic and Static Conditions*, ASCE, Austin, Texas.

Cuelho, E.V., Perkins, S.W. & Ganeshan, S.K. 2005. Determining Geosynthetic Material Properties Pertinent to Reinforced Pavement Design. *Proceedings of the Conference GeoFrontiers, Geotechnical Special Publication 130, Advances in Pavement Engineering*, ASCE, Austin, Texas.

D'Appolonia, D.J., Whitman, R.V. & D'Appolonia, E. 1969. Sand Compaction with Virbratory Rollers. *Journal of Soil Mechanics and Foundations Division, ASCE*, Vol. 95, pp. 263-284.

De Bondt, A.H. 1999. Anti-Reflective Cracking Design of (Reinforced) Asphaltic Overlays, PhD Thesis, Technische Universiteit Delft.

Decoene, Y. 1993. Belgian applications of geotextiles to avoid reflective cracking in pavements. Proc. 2nd Int. RILEM Conf. Reflective Cracking in Pavements, Liege, pp. 391-397.

Duncan J.M., Williams, G.W., Sehn, A.L. & Seed, R.B. 1991. Estimation of Earth Pressures Due to Compaction. *Journal of Geotechnical Engineering*, Vol. 117 (12), pp. 1833-1847.

Duncan, J.M. & Seed, R.B. 1986. Compaction-Induced Earth Pressures under K_o-Conditions. *Journal of Geotechnical Engineering*, Vol. 112 (1), pp. 1-22.

Eiksund, G.R., Hoff, I. & Perkins, S.W. 2004. Cyclic Triaxial Tests on Reinforced Base Course Material. *Proceedings of the Conference EuroGeo 2004*, Munich, Germany, pp. 619-624.

Elsing, A., & Sobolewski, J. 1998. Asphalt-layer polymer reinforcement: long-term experience, new design method, recent developments. *Proc. 5th Int. Conf. Bearing Capacity of Roads and Airfields*, Trondheim, Vol. 3, pp. 1523-1532.

Fannin, R.J. & Sigurdsson, O. 1996. Field Observations on Stabilization of Unpaved Roads with Geosynthetics, *Journal of Geotechnical Engineering*, Vol. 122(7), pp. 544-553.

Francken, L. 1990. Fissuration thermique de structures semi-rigides; essais de simulation. *Proc. 4th Int. RILEM Symp. Mechanical Tests for Bituminous Mixes*, Budapest, pp. 419-431.

Francken, L., & Vanelstraete, A. 1993. On the thermorheological properties of interface systems. *Proc. 2nd Int. RILEM Conf. Reflective Cracking in Pavements*, Liege, pp. 206-219.

Gabr, M., Leng, J. & Ju, T.J. 2001. *Response and Characteristics of Geogrid-Reinforced Aggregate Under Cyclic Plate Load*, Research Report Submitted to Tensar Earth Technologies, NC State University, 40 pp.

Giroud, J.P. & Noiray, L. 1981. Geotextile-Reinforced Unpaved Roads, *Journal of the Geotechnical Engineering Division*, American Society of Civil Engineers, Vol. 107(9), pp. 1233-1254.

GRI 2001. www.geosynthetic-institute.org

Gustafson, K., Said, S., Zarghampour, H., Sandberg, J., Salmenkaita, S., Russwurn, D., Bianco L., Ceschia, C., Lechner, B. & Russiani, M. 2002. *Reinforcement of Flexible road structures with Steel Fabrics to Prolong Service Life. Guidelines*. Reflex Report T9:02, Swedish National Road and Transport Research Institute. 172 p.

Haas R., Wall, J. & Carroll, R.G. 1988. Geogrid Reinforcement of Granular Bases in Flexible Pavements. *Transportation*

Research Record 1188, TRB, National Research Council, Washington DC, USA, pp. 19 – 27.

Haliburton, T.A. & Barron 1983.

Haliburton, T.A., Lawmaster, J.D. & McGuffey, V.C. 1981. *Use of Engineering Fabrics in Transportation Related Applications*, Federal Highway Administration, FHWA DTFH61-80-C-00094.

Hangen, H., Detert, O. & Alexiew, D. 2008. Biaxial Testing of Geogrids: Recent Developments. *Proceedings of the 4th European Geosynthetics Conference EuroGeo4*, Edinburgh Scotland, Paper No. 258.

Haas R., Wall, J. & Carroll, R.G. 1988. Geogrid Reinforcement of Granular Bases in Flexible Pavements. *Transportation Research Record 1188*, TRB, National Research Council, Washington DC, USA, pp. 19 – 27.

Hayden, S.A., Humphrey, D.N., Christopher, B.R., Henry, K.S. & Fetten, C.P. 1999. Effectiveness of Geosynthetics for Roadway Construction in Cold Regions: Results of a Multi-Use Test Section, *Proceedings of the Conference Geosynthetics '99*, Vol. 2, Boston, Massachusetts, March 1999, pp.847-862.

Herbst, G., Kirchknopf, H., & Litzka, J. 1993. Asphalt overlay on crack-sealed concrete pavements using stress distributing media. *Proc. 2nd Int. RILEM Conf. Reflective Cracking in Pavements*, Liege, pp. 425-432.

Holtz, R.D., Christopher, B.R., and Berg, R.R. 2008. *Geosynthetic Design and Construction Guidelines,* Participant Notebook, NHI Course No. 13213, FHWA Publication No. FHWA HI-95-038 (revised), Federal Highway Administration, Washington, DC.

Houlsby, G.T. & Jewell, R.A. 1990. Design of Reinforced Unpaved Roads for Small Rut Depths. *Proceedings of the Fourth International Conference on Geotextiles, Geomembranes and Related Products*, Balkema, The Hague, The Netherlands, Vol. 1, pp. 171-176.

Hufenus, R., Rüegger, R., Weingart, K., Banjac, R., Mayor, P., Springman, S.M., Brönnimann, R. & Feltrin, G. 2004. Reinforcing Foundation Layers on Soft Subgrade, *Proceedings of the Third European Geosynthetics Conference*, Munich, Germany, pp. 255-260.

Huhnholz, M. 1996. Asphalt reinforcement in practice. *Proc. 3rd Int. RILEM Conf. Reflective Cracking in Pavements*, Maastricht, pp. 456-463.

Johansson, S., & Nilsson, L.E. 1998. Steel fabrics as reinforcement in road construction. *Proc. 5th Int. Conf. Bearing Capacity of Roads and Airfields*, Trondheim, Vol. 3, pp. 1513-1522.

Kanerva-Lehto, H. 2009. *Use of steel mesh reinforcements in road structures*. Finnra report 20/2009. Finnra. Helsinki. In Finnish. 80 p.

Kangas, H., Onninen, H. & Saarelainen, S. 2000. *Testing a pavement on thawing, frost-susceptible subgrade with the heavy vehicle simulator*. Finnra report 31/2000, Helsinki 2000, 69 p.

Karam, G. 1993. Experience of Du Pont de Nemours in reflective cracking: site follow up. *Proc. 2nd Int. RILEM Conf. Reflective Cracking in Pavements*, Liege, pp. 370-377.

Kassner, J. 1989. Theory and practical experience with polyester reinforcing grids in bituminous pavement courses. *Proc. 1st Int. RILEM Conf. Reflective Cracking in Pavements*, Liege, pp. 343-349.

Kim, K.W., Doh, Y.S., Lim, S., Rhee, S., & Li, X. 1998. Reinforcement of asphalt pavement to improve resistance against reflection cracking. Proc. 5th Int. Conf. Bearing Capacity of Roads and Airfields, Trondheim, Vol. 3, pp. 1533-1540.

Kinney, T.C. & Barenberg, E.J., 1982, The Strengthening Effect of Geotextiles on Soil-Geotextile-Aggregate Systems, *Proceedings of the Second International Conference on Geotextiles*, Las Vegas, NV, USA, Vol. 2, pp. 347-352.

Kivikoski, H., Pihlajamäki, J. & Tammirinne M. 2002. *Summation report on TPPT test constructions*. Helsinki. Finnra report 8/2002. Helsinki. Finnra. 138 p..

Knapton, J. & Austin, R.A. 1996. Laboratory testing of reinforced unpaved roads, *Earth Reinforcement*, H. Ochiai, N. Yasufuku, and K. Omine eds., Balkema, Rotterdam, The Netherlands, pp. 615-618.

Konietzky, H., te Kamp, L., Gröger, T. & Jenner, C. 2004. Use of DEM to Model the Interlocking Effect of Geogrids Under Static and Cyclic Loading. *Numerical Modeling in Micromechanics via Particle Methods*, A.A. Balkema, Rotterdam, pp. 3-12.

Korkiala-Tanttu, L., Kivikoski, H. & Rathmayer H. 2003a. *The use of steel grid in road test structures. STEELSYNT*. Finnra report 8/2003. Helsinki, Finnra. In Finnish. 41 p.

Korkiala-Tanttu, L. Laaksonen R. & Törnqvist J. 2003b. *Reinforcement of the edge of a steep-sloped pavement HVS-Nordic Heavy Vehicle Simulator test structures.* Finnra Reports 38/2003, Finnra, 46 p.

Kwon, J., Tutumluer, E. & Konietzky, H. 2008. Aggregate Base Residual Stresses Affecting Geogrid Reinforced Flexible Pavement Response. *International Journal of Pavement Engineering*, Vol. 9(4), pp. 275-285.

Laurent, G., & Serfass, J.P. 1993. Comparative sections of reflective crack-preventing systems: four years evaluation. *Proc. 2nd Int. RILEM Conf. Reflective Cracking in Pavements*, Liege, pp. 353-359.

Leng, J. & Gabr, M. 2002. Characteristics of Geogrid-Reinforced Aggregate under Cyclic Load*, Transportation Research Recprd No. 1786*, National Research Council, Washington, D.C., pp. 29-35.

Marchand, J.P. 1993. A crack resistant surface dressing: the results of 8 years of application, and future prospects. *Proc. 2nd Int. RILEM Conf. Reflective Cracking in Pavements*, Liege, pp. 458-463.

McGown, A. & Kupec, J. 2004. A New Approach to the Assessment of the Behavior of Geogrids Subject to Biaxial Loading. *Proceedings of the 3rd European Geosynthetics Conference EuroGeo3*, Munich, Germany, Vol. 2, pp. 643-648.

Miura, N., Sakai, A., Taesiri, Y., Yamanouchi, T. & Yasuhara, K. 1990. Polymer Grid Reinforced Pavement on Soft Clay Grounds. *Geotextiles and Geomembranes*, Vol. 9, pp. 99-123.

Moe, H.L., Watn, A., Aaboe, R., Berntsen, G. & Myhre, Ø. 2008. Norgeospec 2002 - A Nordic System for Specification and Control of Geotextiles in Roads and Other Trafficked Areas. *Proceedings of the Fourth European Geosynthetics Conference*, Edinburgh, Scotland.

Montestruque, G. 2004. Stop of reflective crack propagation with the use of PET geogrid as asphalt overlay reinforcement. *Fifth RILEM International Conference Cracking in Pavement, Mitigation, Risk Assessment and Prevention*. Limoges, France, pp. 231-238.

Montestruque, G. 1996. *Studies of anti-reflective crack systems in asphalt Pavement rehabilitation*. Thesis MSc. Aeronautics Technological Institute, ITA, Brazil.

Montestruque, G., Rodrigues, R., Montez, F.T.M., & Elsing A. 2000. Experimental evaluation of a polyester geogrid as an anti-reflective cracking interlayer on overlays. *Proc. Eurogeo Symp*.Mooney, M.A. & Rinehart, R.V. 2009. In Situ Soil Response to Vibratory Loading and Its Relationship to Roller-Measured Stiffness, *Journal of Geotechnical and Geoenvironmental Engineering*, ASCE. Vol. 135 (8), pp.1022-1031.

Mooney, M.A., Rinehart, R.V., White, D.J., Vennapusa, P.K.R., Facas, N.W. & Musimbi, O.M. 2009. *Intelligent Soil Compaction Systems*. NCHRP Project 21-09, NCHRP, National Academy of Sciences, 269 p.

NCHRP 2003. *NCHRP Project 1-37A, Development of NCHRP 1-37A Design Guide, Using Mechanistic Principles to Improve Pavement Design*, http://www.NCHRP 1-37A Designdesignguide.com/.

NCHRP 2000. *Harmonized Test Methods for Laboratory Determination of Resilient Modulus for Flexible Pavement Design, Volume 1: Unbound Granular Material*. NCHRP Project 1-28a , 198p.

Perkins, S.W. 1999. Mechanical Response of Geosynthetic-Reinforced Flexible Pavements. *Geosynthetics International*, Vol. 6(5), pp. 347-382.

Perkins, S.W. & Eiksund, G.R., 2005. Geosynthetic Material Properties for Use in 2-D Finite Element Pavement Response Models. *Proceedings of the Seventh International Conference on the Bearing Capacity of Roads, Railways and Airfields*, Trondheim, Norway.

Perkins, S.W. & Svanø, G. 2006. Assessment of Interface Shear Growth from Measured Geosynthetic Strains in a Reinforced Pavement Subject to Repeated Loads. *Eighth International Conference on Geosynthetics*, Yokohama, Japan , J. Kuwano & J. Koseki eds., Vol. 3, pp. 813-816.

Perkins, S.W., Christopher, B.R., Cuelho, E.V., Eiksund, G.R., Schwartz, C.S. & Svanø, G. 2009. A Mechanistic-Empirical Model for Base-Reinforced Flexible Pavements. *International Journal of Pavement Engineering*, Vol. 10(2), pp. 101-114.

Perkins, S.W., Christopher, B.R. & Lacina, B.A. 2008. Mechanistic-Empirical Design Method for Unpaved Roads Using Geosynthetics. *Proceedings of the 4th European Geosynthetics Conference EuroGeo4*, Edinburgh Scotland, Paper No. 228.

Perkins, S.W., Christopher, B.R., Eiksund, G.R., Schwartz, C.S. & Svanø, G. 2005. Modeling Effects of Reinforcement on Lateral Confinement of Roadway Aggregate. *Proceedings of the Conference GeoFrontiers*, *Geotechnical Special Publication 130, Advances in Pavement Engineering,* ASCE, Austin, Texas.

Perkins, S.W., Christopher, B.R., Cuelho, E.L., Eiksund, G.R., Hoff, I., Schwartz, C.W., Svanø, G., & Watn, A. 2004. *Development of Design Methods for Geosynthetic Reinforced Flexible Pavements.* U.S. Department of Transportation, Federal Highway Administration, Washington, DC, FHWA Report Reference Number DTFH61-01-X-00068, 263p.

Perrier, H. 1989. Enduits renforces par geotextile sur route en terre: experience Francaise en Guyane. *Proc. 1st Int. RILEM Conf. Reflective Cracking in Pavements*, Liege, pp. 358-363.

Pihlajamäki, J., Wiman L.G. & Gustafson K. 2002. REFLEX Final Report T4:02. Full-Scale Accelerated Tests. Swedish National Road and Transport Research Institute. 58 p.

Sandberg, J. & Björnfot, P. 2004. *Spikfri and bärig väg med stålarmering*. Vägverket.

Sanders, P.J. 2001. *Reinforced Asphalt Overlays for Pavements*, PhD Thesis, University of Nottingham.

Scarpas, A., Blaauwendraad, J., De Bondt, A.H. & Molenaar, A.A.A. 1993. CAPA: a modern tool for the analysis and design of pavements. *Proc. 2nd Int. RILEM Conf. Reflective Cracking in Pavements*, Liege, pp. 121-128

Selig, E.T. 1987. Tensile Zone Effects on Performance of Layered Systems. *Géotechnique*, Vol. 37(3), pp. 247-254.

Schuster, A., & Kuenzer, B. 1989. Polyester and glass fibre geogrids for the prevention of reflective cracking. *Proc. 1st Int. RILEM Conf. Reflective Cracking in Pavements*, Liege, pp. 388-396.

Steen, E.R. 2004. Designing with Geotextiles based on Stress Energy Factors. *Proceedings of the Third European Geosynthetics Conference*, Munich, Germany, pp. 607-610.

Steward, J., Williamson, R. & Mohney, J. 1977. *Guidelines for Use of Fabrics in Construction and Maintenance of Low-Volume Roads*, USDA, Forest Service, Portland, OR. Also reprinted as Report No. FHWA-TS-78-205.

Tang, X., Chehab, G.R. & Palomino, A. 2008. Evaluation of Geogrids for Stabilizing Weak Pavement Subgrade. *International Journal of Pavement Engineering*, Vol. 9(6), pp. 413-429.

Taniguchi, S., & Ikeda, T. 1998. Study in reflective cracking on composite pavement. *Proc. 5th Int. Conf. Bearing Capacity of Roads and Airfields*, Trondheim, Vol. 2, pp. 867-874.

Terzaghi, K. & Peck, R.B. 1967. *Soil Mechanics in Engineering Practice*. John Wiley and Sons, New York.

Thom, N.H. 2003. Grid reinforced overlays: predicting the unpredictable, *Proc. MAIREPAV Conf.*, Guimaraes, Portugal, pp. 317-326

Tsai, W. 1995. *Evaluation of Geotextiles as Separators in Roadways*, Ph.D. Thesis, University of Washington, Seattle, Washington, 172 p.

US Army Corps of Engineers 1999, Test Pilot Study - Chemical Demilitarization Alternative Technology Program (Alt-Tech) Aberdeen Proving Grounds (Edgewood Area), Maryland, U.S. Army Engineer District, Baltimore, February, 93 p.

Uzan, J. 1985. Characterization of Granular Materials. *Transportation Research Record No. 1022*, TRB, National Research Council, Washington DC, USA, pp. 52 – 59.

Walsh, I.D. 1993. Thin overlay to concrete carriageway to minimise reflective cracking. *Proc. 2nd Int. RILEM Conf. Reflective Cracking in Pavements*, Liege, pp. 464-481.

Watn, A., Eiksund, G., Jenner, C. & Rathmayer, H. 2005. Geosynthetic Reinforcement for Pavement Systems: European Perspectives. *Geotechnical Special Publication*, 130-142, *Geo-Frontiers 2005,* American Society of Civil Engineers, Reston, VA, pp. 3019-3037.

Watts, G.R.A., Blackman, D.I. & Jenner, C.G. 2004. The Performance of Reinforced Unpaved Subbases Subjected to Trafficking, *Proceedings of the Third European Geosynthetics Conference*, Munich, Germany, pp. 261 – 266.

Webster, S.L. 1993. *Geogrid Reinforced Base Courses for Flexible Pavements for Light Aircraft: Test Section Construction, Behavior Under Traffic, Laboratory Tests, and Design Criteria*, USAE Waterways Experiment Station, Vicksburg, MS, Technical Report DOT/FAA/RD-92/25, 100 p.

Woon-Hyung K, Edil, T.B., Benson, C.H. & Tanyu, B.F. 2005. Structural Contribution of Geosynthetic-Reinforced Working Platforms in Flexible Pavement. *Transportation Research Record No.1936*, Transportation Research Board of the National Academies Washington, D.C.

Øiseth, E. & Hoff, I. 2006. Use of reinforcement in roads. Proposal for guidelines. SINTEF report 502562-2006.